# INORGANIC NITRATE, HYPOXIA AND THE REGULATION OF CARDIAC MITOCHONDRIAL RESPIRATION – PROBING THE ROLE OF PPARα

James A. Horscroft,[1] Katie A. O'Brien,[1,2] Anna D. Clark,[1] Ross T. Lindsay,[1] Alice Strang Steel,[1] Nathan E.K. Procter,[3] Jules Devaux,[1] Michael Frenneaux,[3] Stephen D.R. Harridge[2] and Andrew J. Murray[1]

[1] Department of Physiology, Development & Neuroscience, University of Cambridge, UK

[2] Centre for Human and Applied Physiological Sciences, King's College London, London, UK

[3] Bob Champion Research and Education Building, University of East Anglia, Norwich, UK

***For correspondence:*** Dr Andrew Murray
Department of Physiology, Development & Neuroscience
University of Cambridge
Downing Street
Cambridge
CB2 3EG
United Kingdom
Telephone: (+44 1223) 333863
Email: ajm267@cam.ac.uk

**Running title:** Nitrate, hypoxia and cardiac mitochondrial function

**Abbreviations**

| | |
|---|---|
| BIOPS | biopsy preservation solution |
| cGMP | cyclic guanosine monophosphate |
| CPT | carnitine palmitoyltransferase |
| CS | citrate synthase |
| eNOS | endothelial nitric oxide synthase |
| ETS | electron transfer system |
| FAO | fatty acid oxidation |
| HADH | 3-hydroxyacyl dehydrogenase |
| HFrEF | heart failure with reduced ejection fraction |
| HIF | hypoxia-inducible factor |
| LDH | lactate dehydrogenase |
| LEAK | leak respiration |
| NO | nitric oxide |
| $NO_2^-$ | nitrite |
| $NO_3^-$ | nitrate |
| NOS | nitric oxide synthase |
| $O_2^{\cdot -}$ | superoxide |
| $ONOO^-$ | peroxynitrate |
| OXPHOS | oxidative phosphorylation |
| PGC1α | peroxisome proliferator-activated receptor gamma co-activator 1α |
| PKG | cGMP-dependent protein kinase G |
| PPAR | peroxisome proliferator-activated receptor |

| | |
|---|---|
| PDH | pyruvate dehydrogenase |
| PDK | pyruvate dehydrogenase kinase |
| ROS | reactive oxygen species |
| sGC | soluble guanylyl cyclase |

**Abstract**

Dietary inorganic nitrate prevents aspects of cardiac mitochondrial dysfunction induced by hypoxia, although the mechanism is not completely understood. In both heart and skeletal muscle, nitrate increases fatty acid oxidation capacity, and in the latter case this involved upregulation of PPARα expression. Here we investigated whether dietary nitrate modifies mitochondrial function in the hypoxic heart in a PPARα-dependent manner. Wild-type and *Ppara*$^{-/-}$ mice were given water containing 0.7 mM NaCl (control) or 0.7 mM $NaNO_3$ for 35 d. After 7 d, mice were exposed to normoxia or hypoxia (10% $O_2$) for the remainder of the study. Mitochondrial respiratory function and metabolism were assessed in saponin-permeabilised cardiac muscle fibres. Environmental hypoxia suppressed mass-specific mitochondrial respiration, and additionally lowered the proportion of respiration supported by fatty acid oxidation by 18% ($P < 0.001$). This switch away from fatty acid oxidation was reversed by nitrate treatment in hypoxic wild-type but not *Ppara*$^{-/-}$ mice, indicating a PPARα-dependent effect. Hypoxia increased hexokinase activity by 33% in all mice, whilst lactate dehydrogenase activity increased by 71% in hypoxic wild-type but not *Ppara*$^{-/-}$ mice. Our findings indicate that PPARα plays a key role in mediating cardiac metabolic remodelling in response to both hypoxia and dietary nitrate supplementation.

200 words (limit 200)

**Key Words:** heart, metabolism, mitochondria, fatty acids, respiration

## Introduction

The mammalian heart is often described as a metabolic omnivore, in reference to its ability to oxidise a variety of substrates in order to meet ATP demands (1). Whilst the healthy heart predominantly uses fatty acid oxidation (FAO) to meet these requirements under fasting conditions, under hypoxic conditions FAO is downregulated in favour of a relative increase in glucose metabolism (2), which requires less $O_2$ per ATP synthesised (1). Key to this response is a reduction in the expression of peroxisome proliferator-activated receptor (PPAR)α, a ligand-activated transcription factor expressed in liver, heart, kidney, and to a lesser extent skeletal muscle (3). When activated, PPARα increases the expression of a number of genes involved in mitochondrial fatty acid import (e.g. *Cpt1b*) and β-oxidation (e.g. *Hadh*, *Acadm*, *Ucp3*) (3). In mice, cardiac-specific ablation of *Arnt*, which encodes hypoxia-inducible factor (HIF)-1β, increased PPARα expression and transcriptional activity, increasing FAO (4), suggesting that HIF signalling attenuates PPARα in hypoxia. Indeed, in cardiomyocytes HIF-1α activation decreased PPARα DNA binding activity (5). In addition to a suppression of FAO, mitochondrial pyruvate oxidation is also suppressed in hypoxia via the phosphorylation of pyruvate dehydrogenase (PDH) by pyruvate dehydrogenase kinase 1 (PDK1), which is induced by HIF-1α in hypoxic cells (6, 7). Thus mitochondrial respiration would be suppressed in favour of glycolytic ATP production.

In the hypoxic rodent heart, the transcriptional activity of PPARα is downregulated in association with a suppression of FAO (8, 9) and an increase in glycolysis (8). As such, the cardiac metabolic phenotype of hypoxic mice resembles that of *Ppara*$^{-/-}$ mice, and notably, no further suppression of FAO occurs in *Ppara*$^{-/-}$ mice following exposure to hypoxia (8). Moreover, whilst hypoxic exposure results in an impaired cardiac energetic reserve in both humans (10) and rodents (8), increasing PPARα activity and FAO in hypoxic mice through a high-fat diet did not improve energetics and in fact worsened contractile function (8), thus it appears that downregulation of FAO in the hypoxic heart is protective. Recent work, however, has suggested that both FAO and energetics might be preserved in hypoxic tissues by dietary supplementation with inorganic nitrate ($NO_3^-$).

Dietary inorganic nitrate ($NO_3^-$) is principally acquired through the consumption of leafy, green vegetables and has effects on mitochondrial function which may be beneficial to human health (11). Nitrate is reduced to nitrite ($NO_2^-$) via oral nitrate reductase in commensal bacteria (12). Nitrite is then converted to nitric oxide (NO) in the stomach by acid

disproportionation (13), and is absorbed into the bloodstream where it can be oxidised to nitrite by ceruloplasmin (14) or to nitrate by haemoglobin (15). Under conditions of moderate hypoxia and/or acidosis, nitrite may be reduced to NO by one of several nitrite reductases, including xanthine oxidoreductase (16), deoxyhaemoglobin (17), deoxymyoglobin (18) and endothelial nitric oxide synthase (eNOS) (19). Under such conditions, endogenous NO production from L-arginine and $O_2$ via the nitric oxide synthase (NOS) enzymes is attenuated due to the low partial pressure of $O_2$, thus nitrate supplementation may prevent a hypoxia-induced fall in NO bioavailability.

A major physiological role of NO is to induce vasodilatation upon its release from the endothelium in response to a range of stimuli (20). NO binds to the haem group of soluble guanylyl cyclase (sGC) inducing cGMP production (21). This in turn activates cGMP-dependent protein kinase G (PKG), which results in smooth muscle relaxation and vasodilatation via a reduction in intracellular [$Ca^{2+}$] (22), thus enhancing blood flow and $O_2$ delivery. Additionally, supplementation with moderate doses of dietary nitrate partially offsets the rise in circulating erythropoietin and haemoglobin in hypoxic rats (23), which might prevent the microcirculatory dysfunction associated with an increased haematocrit (24) further improving $O_2$ delivery. Indeed, native Tibetan highlanders have high levels of plasma nitrate (25) and lower blood haemoglobin concentrations than acclimatised lowlanders at any given altitude (26), and this is associated with superior forearm blood flow (25). Supplementation of dietary nitrate under hypoxic conditions may therefore preserve $O_2$ delivery to respiring tissues.

In addition to effects on $O_2$ delivery though, NO regulates multiple aspects of oxidative metabolism in respiring tissues. NO induces mitochondrial biogenesis through the upregulation of PPARγ co-activator-1α (PGC1α) (27). Within mitochondria, NO competes with $O_2$ at complex IV of the electron transfer system (ETS), leading to partial inhibition of electron transport and control over reactive oxygen species (ROS) signalling (28). NO also reacts with the superoxide ion ($O_2^{\cdot-}$) to form peroxynitrite ($ONOO^-$) (29), which acts as an endogenous toxicant (30). Moreover, NO can induce a post-translational modification of complex I via S-nitrosation, resulting in its inhibition (31), which has implications both for respiratory function and ROS production.

It has been reported that supplementation with dietary nitrate lowers the $O_2$ cost of exercise in humans (32) by increasing mitochondrial thermodynamic efficiency (11), and accordingly

nitrate could be beneficial in hypoxia. In the hypoxic rat heart, nitrate supplementation prevented the downregulation of ETS complex I expression and activity and the depression of mitochondrial FAO, whilst lowering markers of oxidative stress and protecting ATP levels (33). It is not clear, however, whether this nitrate-mediated protection resulted from a direct effect on the cardiomyocyte or through improvements in $O_2$ delivery that offset the challenge of hypoxia. Notably, however, nitrate supplementation enhanced mitochondrial FAO capacity in both the heart (33) and skeletal muscle (34) of normoxic rats. Mechanistically, nitrate increased PPARα transcriptional activity in skeletal muscle, with no increase in FAO seen in *Ppara*$^{-/-}$ mice (34). Moreover, a similar effect on PPARα transcription was seen in cultured myocytes under constant, well-oxygenated conditions (34), suggesting a role for nitrate supplementation beyond any influence of NO on haemodynamics.

Dietary nitrate therefore protects β-oxidation in the hypoxic heart (33), and increases β-oxidation in skeletal muscle via PPARα activation (34). PPARα transcriptional activity is suppressed in the hypoxic rodent heart, although expression of PPARα itself may be unchanged (9). The interaction between nitrate and PPARα in the hypoxic heart, however, remains unclear, and specifically it is not known whether PPARα is essential for the protective effects on mitochondrial respiratory function and FAO elicited by nitrate. We therefore investigated this in wild-type (*Ppara*$^{+/+}$) and *Ppara*$^{-/-}$ mice, exposed to environmental hypoxia or normoxia, with and without supplementation with a moderate concentration of dietary nitrate. We previously reported that nitrate protected aspects of skeletal muscle mitochondrial respiratory function in these mice in hypoxia, and found this occurred independently of PPARα (35). However, it has been suggested that in the skeletal muscle of *Ppara*$^{-/-}$ mice, high expression of PPARβ/δ compensates for the loss of PPARα (36). Moreover, expression of PPARα is higher in heart than skeletal muscle (3). Here we focussed on the role of PPARα in nitrate-mediated effects on the hypoxic heart, hypothesising that nitrate regulates mitochondrial function and β-oxidation in the hypoxic heart in a manner dependent upon PPARα activity.

## Materials and Methods

Animal work was carried out in accordance with UK Home Office regulations under the Animals in Scientific Procedures Act, and underwent review by the University of Cambridge Animal Welfare and Ethical Review Committee. Procedures involving live animals were carried out by a licence holder in accordance with these regulations.

### *Study design*

The overall study design has been described previously (35). Mice were bred on a pure 129Ev/Sv background with 10 backcrosses. The original breeding pairs of wild-type (*Ppara*$^{+/+}$) and *Ppara*$^{-/-}$ mice were a kind gift of Frank Gonzalez (National Institutes of Health, Bethesda, MD). Mice were housed in a temperature, humidity and light controlled environment (23°C) from birth with a 12 h/12 h light/dark cycle. Normoxic mice were housed under the same environmental conditions as those in the hypoxia chamber. Mice were provided with a standard quality-controlled diet RM1(E) (65.0% carbohydrate, 13.1% crude protein, 3.5% crude fat, 10 mg/kg nitrate, trace nitrite, Special Diet Services) and distilled water *ad libitum*. At six weeks of age, mice from each genotype were randomly assigned to receive sodium chloride (0.7 mM) as a control or sodium nitrate (0.7 mM $NaNO_3$) in their drinking water. After a further 7 d, mice from each genotype/treatment combination were equally and randomly assigned to remain under normoxic conditions (21% $O_2$) or transferred to hypoxic (10% $O_2$) conditions in a hypoxia chamber (PFI Systems Ltd., Milton Keynes, UK). Mice were maintained under these conditions for 28 d (Fig. 1). Body mass, food intake and water intake was measured weekly.

Mice were killed 80 ± 4 d after birth by dislocation of the neck. The chest cavity was opened and the heart removed and immediately placed in ice-cold biopsy preservation medium (BIOPS), comprising 2.77 mM $CaK_2EGTA$, 7.23 mM $K_2EGTA$, 6.56 mM $MgCl_2.6H_2O$, 20 mM taurine, 15 mM phosphocreatine, 20 mM imidazole, 0,5 mM dithiothreitol, 50 mM MES, 5.77 mM $Na_2ATP$, pH 7.1. The heart was blotted and trimmed of extraneous tissue before being separated into three sections: the apex was kept in ice-cold BIOPS for high-resolution respirometry, while the middle section and base were snap-frozen in liquid nitrogen. Meanwhile, a droplet of blood was collected from the tail vein and loaded into a microcuvette to quantify blood-haemoglobin concentration ($[Hb]_b$) using a HemoCue Hb 201 Analyzer (Quest Diagnostics, Sweden).

***High-resolution respirometry***

Muscle fibre bundles were dissected from the heart and permeabilised using saponin as described previously (37). Mitochondrial respiratory function was assessed at 37°C using an Oxygraph-2K (Oroboros Instruments, Innsbruck, Austria) in respiratory medium comprising 0.5 mM EGTA, 3 mM $MgCl_2.6H_2O$, 20 mM taurine, 10 mM $KH_2PO_4$, 20 mM HEPES, 1 mg/ml BSA, 60 mM K-lactobionate, 110 mM sucrose, pH 7.1. Respiratory medium was hyperoxygenated at the start of each experiment and periodically throughout each assay by lifting the stopper of the oxygraph chamber slightly to introduce a gas phase, before injecting pure $O_2$ gas into the gas phase and then re-sealing the chamber once the desired $O_2$ concentration was reached. $O_2$ concentration in the chambers was thus maintained between 250 and 500 μM in order to negate limitations associated with $O_2$ diffusion (37) and all reported respiratory fluxes were recorded within this range.

Two substrate-inhibitor titration assays were performed to investigate respiratory control of different components of the mitochondrial system (Table 1). Assay 1 was based on a previously described protocol (38) with the concentrations optimised for permeabilised cardiac fibres, and was designed to investigate β-oxidation of fatty acids. Assay 2 was adapted from a previously described protocol (39) and aimed to characterise control of different substrate-supported pathways over oxidative phosphorylation.

*Assay 1*

The addition of malate (2 mM), plus substrates for carnitine palmitoyltransferase 1 (CPT1), palmitoyl coenzyme A (40 μM) and carnitine (5 mM), resulted in LEAK respiration constrained by the activity of CPT1 ($CPT1_L$). ADP (10 mM) resulted in oxidative phosphorylation (OXPHOS) also constrained by CPT1 ($CPT1_P$). In order to bypass CPT1 and investigate β-oxidation capacity ($PalM_P$), palmitoyl carnitine (20 μM) was added. Finally, cytochrome *c* (10 μM) was added to assess the integrity of the outer mitochondrial membrane.

*Assay 2*

Administration of octanoyl carnitine (0.2 mM) with malate (2 mM) resulted in LEAK respiration ($OctM_L$). ADP (10 mM) addition resulted in OXPHOS respiration dependent on β-oxidation of medium chain fatty acids ($OctM_P$). Pyruvate (5 mM) was then added ($PM_P$), followed by glutamate (10 mM) to support electron flux through the N-pathway via complex

I ($GM_P$). Succinate (10 mM) was then administered to additionally support electron flux through the S-pathway via complex II ($GMS_P$). Following this, cytochrome *c* (10 μM) was added to assess mitochondrial membrane integrity, before rotenone (0.5 μM) was administered to inhibit complex I and restrict electron flux to the S-pathway via complex II ($S_P$).

*Coupling control ratios*

In both assays, the OXPHOS coupling efficiency (*j*), i.e. the proportion of OXPHOS capacity that could not be explained by leak-limited respiration, was calculated as follows:

$$j = \frac{P - L}{P}$$

*j* OXPHOS coupling efficiency

*L* LEAK respiration rate

*P* OXPHOS respiration rate

Equation 1. OXPHOS coupling efficiency

*Substrate control ratios*

The control of CPT1 over β-oxidation was assessed from Assay 1, by expressing CPT1-limited OXPHOS as a ratio of β-oxidation-limited OXPHOS:

$$\mathrm{FCR}_{CPT1} = \frac{\mathrm{CPT1}_P}{\mathrm{PalM}_P}$$

Equation 2. Flux control of CPT1 over β-oxidation

From Assay 2, OXPHOS supported by the F-Pathway (via β-oxidation), the N-pathway (via complex I) and the S-pathway (via complex II) were expressed as a ratio of maximal OXPHOS to discern the proportion of oxygen flux controlled by these pathways as follows:

$$\mathrm{FCR}_F = \frac{\mathrm{OctM}_P}{\mathrm{GMS}_P}$$

Equation 3. Flux control of F-pathway (via β-oxidation) over OXPHOS

$$\mathrm{FCR}_N = \frac{\mathrm{GM}_P}{\mathrm{GMS}_P}$$

Equation 4. Flux control of N-pathway (via complex I) over OXPHOS

$$\mathrm{FCR}_S = \frac{\mathrm{S}_P}{\mathrm{GMS}_P}$$

Equation 5. Flux control of S-pathway (via complex II) over OXPHOS

Finally, the ratio of OXPHOS supported by octanoyl carnitine and malate to OXPHOS supported by pyruvate and malate in Assay 2 was used as an indicator of the relative capacity for fatty acids as a substrate for mitochondrial respiration:

$$\mathrm{FCR}_{FA/P} = \frac{\mathrm{OctM}_P}{\mathrm{PM}_P}$$

Equation 6. OXPHOS capacity for fatty acid oxidation relative to pyruvate oxidation

***Enzyme activity assays***

Cardiac muscle homogenates were prepared from the contents of the oxygraph chamber. In brief, the entire contents of each chamber were removed and the chambers washed with 2 ml respiratory medium. The original contents and wash were combined with 2 µl protease inhibitor (cOmplete Protease Inhibitor Cocktail, Roche) and 40 µl Triton X-100 (1%). The solution was then homogenised using a Polytron (25,000 rpm, 30 sec) (PT-10-35 GT Kinematic Inc., Switzerland). The homogenate was centrifuged (10,000 rpm, 10 min, 4˚C) and the supernatant removed and stored at -80˚C until use.

In addition, whole tissue homogenates were prepared. Approximately 10 mg of cardiac muscle from the mid-section of the heart was homogenised with an Eppendorf pestle in an Eppendorf tube containing 300 µl of homogenisation buffer (20 mM HEPES, 1 mM EDTA, 0.1% Triton X-100, pH 7.2). The samples were then centrifuged (1,000 × *g*, 30 s, 4°C) and the supernatant collected.

Protein concentration of chamber and tissue homogenates was measured using the Quick Start Bradford protein assay (Bio Rad).

Enzyme activity assays were carried out at 37°C using an Evolution 220 spectrophotometer (Thermo Scientific). Cardiac citrate synthase activity was quantified using a method described previously (40) with a sample size of 10 µg protein. The assay buffer contained 20 mM Tris, 5,5’dithiobis2-nitrobenzoicacid and 0.3 mM acetyl CoA, pH 8.0. The reaction was initiated by the addition of 0.5 mM oxaloacetate and absorbance change at 412 nm was measured.

Activity of the β-oxidation enzyme 3-hydroxyacyl dehydrogenase (HADH) was measured as described previously (41) with a sample size of 20 μg protein. The assay buffer contained 50 mM imidazole, 0.15 mM NADH and 0.1% Triton X-100, pH 7.4 Recording of absorbance change at 340 nm was initiated 10 s after addition of 0.1 mM acetoacetyl coenzyme A.

Hexokinase activity was measured with a sample size of 60 μg protein as described previously (42). The assay buffer contained 20 mM imidazole, 1 mM ATP, 5 mM $7H_2O$.MgCl, 5 mM dithiothreitol (DTT), 2 mM $NAD^+$ and 3.125 U glucose-6-phosphate dehydrogenase, pH 7.4. Recording of absorbance change at 340 nm was initiated 10 s after addition of 5 mM glucose.

Activity of lactate dehydrogenase (LDH) was quantified essentially as described previously (41) with a sample size of 2 μg protein. The assay buffer contained 50 mM HEPES and 0.3 mM NADH, pH 7.0. Recording of absorbance change at 340 nm was initiated 10 s after addition of pyruvate.

***Pyruvate dehydrogenase expression and phosphorylation***

Samples of left ventricle that had been snap frozen in liquid nitrogen were added to 100-150 μl NP40 cell lysis buffer (ThermoFisher Scientific, US) containing Halt™ protease and phosphatase inhibitor cocktail (ThermoFisher Scientific, US). Samples were manually crushed then homogenised on ice using a Pellet Pestle (Sigma-Aldrich, UK). Homogenates were then snap frozen using liquid nitrogen and allowed to thaw on ice, after which they were homogenised for a second time. Samples underwent a further two freeze thaw cycles using liquid nitrogen, vortexing each time, before centrifugation at 16,700 x *g* for 10 min at 4°C. Supernatants were collected and stored at -80°C. Protein concentration was determined using the Bio-Rad DC Assay (Bio-Rad, US). Samples were loaded into Laemmli buffer at a concentration of 1.5 mg/ml and underwent SDS-PAGE using 10% acrylamide gels under reducing conditions for approximately 1 h at 0.08 A, after which they were transferred onto PVDF membrane (GE Healthcare, UK) for approximately 1.5 h at 0.38 A. Membranes were subsequently blocked for a minimum of 2 h in either 5% (w/v) bovine serum albumin or skimmed milk in TBS-T, as appropriate. Primary antibody targets were Phospho(serine 232)-PDH (1:2000, Calbiochem), Phospho(serine 293)-PDH (1:1000, Abcam), Phospho(serine 300)-PDH (1:1000, Calbiochem), PDH (1:1000, Cell Signaling Technology), and β-actin (1:5000, Sigma). Secondary detection was carried out using HRP-conjugated goat anti-rabbit (1:1000, Cell Signaling Technology) or goat anti-mouse (1:1500, Dako) antibodies.

Membranes were developed using Pierce™ ECL western blotting substrate (ThermoFisher Scientific, US) and images captured using a ChemiDoc-It2 imager (Ultra-Violet Products Ltd, US) with VisionWorksLS 8.1.2. software (Ultra-Violet Products Ltd, US). Images were analysed using ImageJ and normalised to β-actin expression.

### *Statistics*

In order to investigate the individual effects of hypoxic exposure, dietary nitrate and *Ppara*$^{-/-}$ and the interactions between these effects, a three-way analysis of variance (ANOVA) was performed. The statistical approach used has been described previously (43). Initially, the three-way interaction was considered for significance. If there was a significant three-way interaction, main effects and two-way interactions were disregarded and a post-hoc Tukey's HSD test performed. Pairwise comparisons of groups between which only one of the independent variables differed were considered, and the results recorded. If the three-way interaction was not significant but one or more two-way interactions were significant, a post-hoc Tukey's HSD test was performed to investigate each two-way interaction. Any main effects of variables involved in the significant two-way interaction(s) were not considered, while main effects of variables not involved in significant interactions were. In instances where no three-way or two-way interactions were significant, the main effects of all three independent variables were considered. Main effects combine all four groups in each state of one independent variable and make a pairwise comparison between these combinations (e.g. all four wild-type vs. all four *Ppara*$^{-/-}$ groups). All analyses were carried out using R software (The R Foundation for Statistical Computing) and $P$ values $< 0.05$ were considered significant.

Graphs were generated using GraphPad Prism 7 software and follow a colour/pattern scheme whereby white indicates normoxia (21% $O_2$), blue hypoxia (10% $O_2$), block colour chloride ($Cl^-$) and striped nitrate ($NO_3^-$) treated groups. In addition the wild type groups are separated from the *Ppara*$^{-/-}$ groups. Graphs display results as mean +/- SEM. Statistically significant differences between groups are indicated in black (differences between genotypes), blue (differences between normoxia and hypoxia) and orange (interactions linked to nitrate treatment vs chloride).

## Results

### *Animal data*

Body mass, blood haemoglobin, and food, water and nitrate intake have been reported previously for these mice (35).

Briefly, food and water intake fell in hypoxic mice in Week 2 (the first week of hypoxic exposure). Food intake recovered in hypoxic animals over subsequent weeks, such that it was the same in all groups at the end of the study. Water intake recovered more quickly than food intake, and was the same in all groups from Week 3 onwards. Inorganic nitrate intake calculated from food and water intake and over the course of the study was 153 - 257 μmol/kg/d in nitrate-treated mice, compared with 18 - 31 μmol/kg/d in chloride-treated mice

Body mass was the same in all wild-type mice at the start of the study, but *Ppara*$^{-/-}$ mice were 6% lighter than wild-types. At the end of the study, *Ppara*$^{-/-}$ mice were 5% lighter than wild-types ($P < 0.01$, PPARα main effect), whilst hypoxic mice were 4% lighter than normoxic mice ($P < 0.001$, hypoxia main effect) and nitrate-treated mice were 3% lighter than chloride-treated mice ($P < 0.05$, nitrate main effect). Blood haemoglobin concentration, measured at the end of the study, was higher in hypoxic mice than normoxic mice (35).

### *Cardiac mitochondrial respiration*

#### *Mass-specific respiration*

Assay 1 was used to measure aspects of FAO and the control exerted by CPT1, with respiration rates initially normalised to wet weight of tissue (Fig. 2). Mass-specific respiration rates in *Ppara*$^{-/-}$ mice were 10% ($P < 0.01$, Fig. 2A), 23% ($P < 0.001$, Fig. 2B) and 27% lower ($P < 0.001$, Fig. 2C, all PPARα main effect) when limited by proton leak ($CPT1_L$), CPT1 flux ($CPT1_P$) and β-oxidation ($PalM_P$), respectively. Hypoxic exposure resulted in 11% lower LEAK respiration ($P < 0.01$, Fig. 2A) and 13% lower OXPHOS supported by β-oxidation ($P < 0.05$, Fig. 2C, both hypoxia main effect). Taken together, these data confirm that PPARα supports FAO in the mouse heart, whilst hypoxia suppresses the mass-specific capacity for β-oxidation.

Assay 2 was used to measure respiration supported by FAO and substrates for the N-pathway via Complex I and the S-pathway via Complex II of the ETS, with respiration rates initially normalised to wet weight of tissue (Fig. 3). All respiration rates were lower in *Ppara*$^{-/-}$ mice

compared with wild-types, and in hypoxic mice compared with normoxic mice, whilst dietary nitrate supplementation had no effect on mass-specific respiration rates.

In *Ppara*$^{-/-}$ mice, LEAK respiration ($OctM_L$) and OXPHOS respiration ($OctM_P$) supported by malate and octanoyl carnitine were 21% lower ($P < 0.001$, Fig. 3A) and 45% lower ($P < 0.001$, Fig. 3B, both PPARα main effect) than in wild-type mice, underlining the role of PPARα in regulating cardiac fatty acid oxidation. Meanwhile, OXPHOS supported by pyruvate and malate ($PM_P$) was 16% lower ($P < 0.001$, Fig. 3C), by glutamate and malate ($GM_P$) was 14% lower ($P < 0.001$, Fig. 3D), by glutamate, malate and succinate ($GMS_P$) was 9% lower ($P < 0.01$, Fig. 3E) and by succinate following the addition of rotenone ($S_P$) was 10% lower ($P < 0.01$, all PPARα main effect, Fig. 3F).

In hypoxic mice, $OctM_L$ and $OctM_P$ were 16% ($P < 0.001$, Fig. 3A) and 17% ($P < 0.001$, Fig. 3B) lower than in normoxic mice, whilst $PM_P$ was 10% lower ($P < 0.01$, Fig. 3C), $GM_P$ was 10% lower ($P < 0.01$, Fig. 3D), $GMS_P$ was 10% lower ($P < 0.01$, Fig. 3E) and $S_P$ was 13% lower ($P < 0.01$, Fig. 3F, all hypoxia main effect).

Together, these data show that both *Ppara* ablation and hypoxic exposure lower oxidative capacity in the mouse heart, with suppression of fatty acid-supported respiration occurring to a greater extent than respiration supported by other substrates. This is particularly pronounced in the case of *Ppara* ablation.

*Citrate synthase-specific respiration*

Both hypoxic exposure and *Ppara*$^{-/-}$ resulted in a general lowering of mass-specific respiration rates in mouse heart. This might be attributable to a loss of cardiac mitochondrial content or to changes in respiration per mitochondrial unit, and therefore to further probe the effects of hypoxia, nitrate and PPARα on mitochondrial respiration, we extracted the contents of the oxygraph chambers and measured the activity of citrate synthase (CS) in chamber homogenates. CS activity is a putative marker of mitochondrial content (44), and by expressing mitochondrial respiration rates relative to CS activity we were able to consider respiratory capacities per mitochondrial unit.

In Assay 1, hypoxia had no effect on any CS-corrected respiration rate (Fig. 4). Dietary nitrate supplementation increased $CPT1_L$ by 38% ($P < 0.01$, Fig. 4A), $CPT1_P$ by 33% ($P < 0.05$, Fig. 4B) and $PalM_P$ by 36% ($P < 0.01$, Fig. 4C, all Tukey's test of nitrate/PPARα interaction) in wild-type but not *Ppara*$^{-/-}$ mice. *Ppara* knockout lowered all CS-corrected

respiration rates. In normoxic mice, *Ppara* knockout lowered $CPT1_L$ by 25% ($P < 0.05$, Fig. 4A), $CPT1_P$ by 38% ($P < 0.001$, Fig. 4B) and $PalM_P$ by 38% ($P < 0.001$, Fig. 4C, all Tukey's test of hypoxia/PPARα interaction). In nitrate-supplemented mice, *Ppara* knockout lowered $CPT1_L$ by 23% ($P < 0.05$, Fig. 4A), $CPT1_P$ by 34% ($P < 0.001$, Fig. 4B) and $PalM_P$ by 35% ($P < 0.001$, Fig. 4C, all Tukey's test of nitrate/PPARα interaction). Taken together, these data suggest that *Ppara* ablation attenuates fatty acid oxidation capacity per mitochondrial unit, and that nitrate increases fatty acid oxidation per mitochondrial unit in a PPARα-dependent manner.

In Assay 2, neither nitrate supplementation nor hypoxic treatment affected CS-corrected respiration rates (Figure 5). *Ppara* ablation, however, lowered CS-corrected $OctM_L$ by 25% ($P < 0.01$, Fig. 5A), $OctM_P$ by 27% ($P < 0.001$, Fig. 5B), $PM_P$ by 19% ($P < 0.05$, Fig. 5C) and $GM_P$ by 17% ($P < 0.05$, Fig. 5D, all PPARα main effect). $GMS_P$ and $S_P$ were unaffected by nitrate, hypoxia or genotype (Fig. 5E and 5F). These data further support the notion that *Ppara* ablation attenuates cardiac mitochondrial fatty acid oxidation capacity, in addition to any effect on mitochondrial content.

*OXPHOS coupling efficiency*

OXPHOS coupling efficiency, indicating the increase in respiration following addition of ADP relative to the resulting respiration rate was calculated for both assays (Supplementary Fig. 1). In Assay 1 and Assay 2, OXPHOS coupling efficiency was 19% and 29% lower, respectively, in *Ppara*$^{-/-}$ mice compared with wild-type mice ($P < 0.001$, PPARα main effect). Neither nitrate-supplementation nor hypoxic exposure affected OXPHOS coupling efficiency. This data suggests that whilst PPARα enhanced fatty acid-supported respiration in both LEAK and OXPHOS states, the effect on the OXPHOS state was proportionally greater.

*Substrate control ratios*

To further investigate the effects of nitrate-supplementation, hypoxic-exposure and PPARα on cardiac mitochondrial respiration, and the interactions between these three factors, we used substrate control ratios to interrogate control points and substrate-led pathways (Fig. 6).

Firstly, to understand the effect of these factors on the activity of CPT1 (an enzyme responsible for the entry of long chain fatty acid substrates into mitochondria via the addition of carnitine) we expressed $CPT1_P$ relative to $PalM_P$ ($FCR_{CPT1}$, Fig. 6A). Here we found that the substrate control ratio was unaffected by any factor, indicating that whilst in *Ppara*$^{-/-}$ mice

and hypoxic mice OXPHOS supported by CPT1 substrates and β-oxidation are suppressed, the effects on these two respiration rates are proportionally similar.

Next, we sought to understand the contribution of three substrate-led pathways to total OXPHOS capacity, expressing OXPHOS supported by a) the F-pathway via β-oxidation ($OctM_P$), b) the N-pathway via complex I ($GM_P$) and c) the S-pathway via complex II ($S_P$), relative to maximal OXPHOS ($GMS_P$).

In wild-type, but not *Ppara*$^{-/-}$ mice, exposure to hypoxia lowered OXPHOS respiration through the F-pathway relative to maximal OXPHOS ($FCR_F$) by 32% ($P < 0.001$, Tukey's test of hypoxia/PPARα interaction, Fig. 6B). Similarly, this was 41% lower in normoxic *Ppara*$^{-/-}$ mice compared with wild-type mice. This suggests that hypoxic exposure lowers fatty acid oxidation, relative to maximal OXPHOS, in a PPARα-dependent manner.

OXPHOS supported by the N-pathway via complex I, relative to maximal OXPHOS ($FCR_N$), was 7% lower in *Ppara*$^{-/-}$ mice compared with wild-type mice ($P < 0.001$, PPARα main effect, Supplementary Fig. 2A) but was unaffected by hypoxic exposure or nitrate supplementation. Meanwhile, OXPHOS supported by the S-pathway via complex II ($FCR_S$), was unaffected by *Ppara* ablation or hypoxia, but was 2% higher in nitrate-supplemented mice ($P < 0.05$, nitrate main effect, Supplementary Fig. 2B).

Finally, we expressed octanoyl carnitine-supported OXPHOS ($OctM_P$) relative to pyruvate-supported OXPHOS ($PM_P$) in order to indicate the relative capacity for FAO compared with pyruvate-linked respiration through the N-pathway ($FCR_{Oct/P}$, Fig. 6C). The relative capacity for FAO was decreased by hypoxia in chloride-supplemented wild-type mice by 18% ($P < 0.001$, Tukey's test of nitrate/hypoxic/PPARα interaction) but not in nitrate-supplemented wild-type mice nor in either group of hypoxic *Ppara*$^{-/-}$ mice. Dietary nitrate reversed this effect in hypoxic wild-type mice, increasing the relative capacity for FAO by 17% ($P < 0.05$, Tukey's test of nitrate/hypoxia/PPARα). Again, no effect was seen in *Ppara*$^{-/-}$ mice. The relative capacity for FAO was, however, lower in *Ppara*$^{-/-}$ mice ($P < 0.001$, Tukey's test of nitrate/hypoxia/PPARα interaction). These data therefore demonstrate that in mouse heart (i) *Ppara* ablation induces a substrate switch away from fatty acids, (ii) exposure to hypoxia induces a substrate switch away from fatty acids acting via decreased PPARα activity, and (iii) dietary nitrate prevents the hypoxia-induced substrate switch in a PPARα-dependent manner.

***Enzyme activities***

Hypoxic exposure resulted in 32% lower citrate synthase activities in wild-type mouse hearts compared with those of their normoxic counterparts ($P < 0.05$, Tukey's test of hypoxia/PPARα interaction) but did not affect CS activity in *Ppara*$^{-/-}$ mice (Fig. 7A).

Nitrate-supplemented wild-type mice had 33% higher activities of the β-oxidation enzyme HADH in heart ($P < 0.01$), whilst no effect was seen in *Ppara*$^{-/-}$ mice (Fig. 7B). Moreover, in *Ppara*$^{-/-}$ mice supplemented with nitrate, but not by chloride, HADH activity was 35% lower than in wild-type counterparts ($P < 0.01$, Tukey's test of nitrate/PPARα interaction). This suggests that dietary nitrate increases HADH activity in cardiac tissue via a PPARα-dependent mechanism.

Hexokinase activity was 33% higher in hypoxic groups, relative to normoxic counterparts ($P < 0.001$, hypoxia main effect), with no significant effect on hexokinase activity resulting from nitrate supplementation or genotype (Fig. 7C). Hypoxia also increased LDH activity by 71% in wild-type, but not *Ppara*$^{-/-}$ mice ($P < 0.001$, Tukey's test of hypoxia/PPARα interaction, Fig. 7D). Hypoxia was also permissive of a PPARα effect, since under hypoxic but not normoxic conditions *Ppara* ablation resulted in 50% lower LDH activities ($P < 0.001$, Tukey's test of hypoxia/PPARα interaction). Dietary nitrate did not affect the activity of either hexokinase or LDH. Thus, hypoxia increased hexokinase activity in a manner that was independent of dietary nitrate and PPARα, but increased LDH in a manner that was dependent upon PPARα.

***Pyruvate dehydrogenase levels and phosphorylation***

To examine the regulation of pyruvate oxidation, total and phosphorylated PDH levels were measured in cardiac homogenates by immunoblotting. There was no specific effect of hypoxia on total PDH levels (Fig 8A), although total levels were higher in hypoxic nitrate-supplemented wild-type mice compared with their normoxic counterparts ($P < 0.05$, Tukey's test of hypoxia/nitrate/PPARα interaction). Hypoxia increased phosphorylation of PDH at serine residues 232, 293 and 300 in wild-type mice, and this was prevented by nitrate supplementation ($P < 0.01$, Tukey's test of hypoxia/nitrate/PPARα interaction, Fig 8B-D). There was no clear effect of hypoxia on phosphorylation of any serine residue in *Ppara*$^{-/-}$ mice. At serine 232, nitrate supplementation appeared to enhance phosphorylation in hypoxic *Ppara*$^{-/-}$ mice ($P < 0.05$, Tukey's test of hypoxia/nitrate/PPARα interaction, Fig 8B). Overall,

these data suggest hypoxia increases PDH inhibition by phosphorylation in a PPARα-dependent manner, whilst nitrate prevents this.

## Discussion

We have previously demonstrated that a moderate dose of dietary nitrate protects mitochondrial respiratory function, FAO and energetics in the hypoxic rat heart (33), and enhances skeletal muscle FAO capacity through a mechanism dependent upon activation of PPARα (34). Decreased PPARα transcriptional activity appears to be a key aspect of the cardiac metabolic response to hypoxia (8, 9), so here we sought to understand whether PPARα plays a role in mediating the protective effect of nitrate in the hypoxic heart.

We found that hypoxic exposure was associated with the suppression of mass-specific respiratory capacity and citrate synthase activity in mouse heart, with no protective effect of nitrate. Mass-specific respiration was also lower in *Ppara*$^{-/-}$ mice compared with wild-type mice. Hypoxia increased phosphorylation of PDH in wild-type mice, and also increased the capacity for glycolysis with increased hexokinase activity in all mice and increased LDH activity in wild-type mice. In addition to the general suppression of oxidative capacity, hypoxia resulted in a particular downregulation of FAO capacity in wild-type mice. This was reversed by nitrate treatment, an effect not apparent in *Ppara*$^{-/-}$ mice. Similarly, nitrate increased activity of HADH in wild-type mice, but not *Ppara*$^{-/-}$ mice.

Strengths of this study include the use of high-resolution measurements of oxygen flux to consider multiple aspects of FAO capacity with both CPT1-dependent and independent substrates. Our inclusion of both mass-specific and mitochondrial-specific FAO capacity measurements, as well as FAO in proportion to maximal OXPHOS capacity is also a strength. It should be noted, however, that all measurements were carried out under conditions where oxygen and substrates were saturating, and whilst our data indicate alterations in respiratory capacity there may be further, subtle differences in mitochondrial respiration *in vivo* at physiological oxygen and substrate concentrations that we have not measured here. The use of permeabilised fibres, rather than isolated mitochondria, allowed us to measure respiration in the entire population of cardiac mitochondria, albeit without allowing us to distinguish between effects on the interfibrillar and subsarcolemmal populations of mitochondria (45). A further strength of this study was the statistical approach, which, whilst complex, allowed us to directly address the key hypothesis that nitrate exerts effects in hypoxia acting through PPARα. The three-way ANOVA approach allowed us to test the interaction between these three factors, and represented a conservative approach, eliminating the need for multiple comparisons and strengthening the conclusions of this

study. This approach, however, does increase the chance of type 2 errors and is not suitable for testing differences between just two of the groups, e.g. the effect of hypoxia on wild-type (non-nitrate-supplemented) mice, for which a more targeted study design would be more appropriate.

The use of mice, rather than rats, is both a strength and a weakness of this study. The *Ppara*$^{-/-}$ mouse has been studied extensively, particularly in relation to the role of PPARα in regulating FAO in various tissues, and was a valuable component of this study. Mice, however, differ from rats and humans, in their NO production rates (46) and concentrations of circulating nitrate/nitrite levels (47). Moreover, we only used male mice in this study, which may be a limitation since, for example, gender dimorphic differences in the anti-platelet response to nitrate supplementation have been observed in humans (48). As with our previous studies, we were able to precisely control nitrate intake using a standardised quality-controlled diet and deionised water (23, 33-35, 49, 50). Whilst the anorexic effects in the early stages of hypoxic exposure may have confounded our findings, the long duration of the hypoxic exposure proved to be a strength since water intake and therefore nitrate intake stabilised in hypoxic mice by week 2, matching that of their normoxic counterparts for the remainder of the study.

Unlike our previous findings in rat heart (33), however, we saw no protective effect of nitrate supplementation on mass-specific oxidative phosphorylation. This could be due to species differences, indeed 17 months of $NaNO_3$ supplementation at 1 mM did not alter plasma nitrate concentration in mice (51), whilst 0.7 mM $NaNO_3$ increased circulating nitrate in rats (33). It should be noted, however, that both the duration (4 weeks) and degree of hypoxia (10% $O_2$) were more severe in this study than in our previous work (2 weeks at 13% $O_2$), and this may have limited the effectiveness of nitrate supplementation. Of note, the increased activity of LDH is an established hypoxia response in heart (52) and this was seen in both chloride-supplemented and nitrate-supplemented mice, perhaps suggesting that nitrate supplementation didn't fully restore $O_2$ delivery to these hearts.

The general suppression of mass-specific respiratory capacity, particularly in the context of more prolonged and severe hypoxia, might be explained by a loss of mitochondrial content in these hearts. Indeed we saw that hypoxia lowered CS activity in the hearts of wild-type mice in this study, whilst there was no such change in CS in our previous study which employed a milder hypoxia protocol (33). In skeletal muscle, the suppression of CS is dependent on both

duration and degree of hypoxia (53). CS activity is a putative marker of mitochondrial density, correlating with mitochondrial volume in the skeletal muscle of healthy, young adult humans (44) although whether this correlation holds in the mouse heart under all conditions described here is unknown.

In addition to the general effect of hypoxia on mass-specific respiration, a particular suppression of FAO was seen. This was indicated by a fall in CS-corrected respiration rates for fatty acid substrates, and also by substrate control ratios expressing FAO as a proportion of maximal OXPHOS or in relation to pyruvate-supported OXPHOS. This effect of hypoxia was seen in the hearts of wild-type but not *Ppara*$^{-/-}$ mice, indicating that the hypoxic suppression of FAO is primarily driven by decreased PPARα activity, as suggested previously (8). There was no specific effect on CPT1-supported FAO (with palmitoyl-CoA plus malate) compared with CPT1-independent respiration (with palmitoyl carnitine plus malate), indicating that whilst CPT1 activity may be downregulated there are also effects of a similar magnitude downstream, probably on β-oxidation capacity, although in agreement with our previous work (9) HADH activity was unaltered by hypoxia. Whilst the severity of the hypoxic stimulus used here may have prevented any restorative effect of nitrate on mass-specific respiration, nitrate did prevent the particular suppression of FAO, but only in wild-type mice, suggesting that PPARα is necessary for these nitrate-mediated effects to occur. Moreover, nitrate-supplementation increased HADH activity in the hearts of wild-type mice, but not *Ppara*$^{-/-}$ mice.

In addition to the effect of hypoxia, mass-specific respiratory capacity was lower in the hearts of *Ppara*$^{-/-}$ mice than those of wild-type mice, and as might be expected this was most pronounced for respiration rates supported by fatty acid substrates, although a suppression of respiration supported by substrates for the N-pathway via complex I (pyruvate, glutamate and malate) and the S-pathway via complex II (succinate) was also seen. When corrected for CS activity, respiration supported by fatty acid substrates remained lower in *Ppara*$^{-/-}$ mice compared with wild-type mice, underlining its importance in regulating cardiac FAO, but of note respiration supported by N-pathway substrates was also was lower in *Ppara*$^{-/-}$ mice. Unlike in wild-type mice, there was no effect of nitrate supplementation on FAO capacity or HADH activity in *Ppara*$^{-/-}$ mice, demonstrating that in line with our initial hypothesis, PPARα is an essential mediator of the effects of nitrate on cardiac metabolism in hypoxia.

Activities of hexokinase and LDH were increased following hypoxia as did PDH phosphorylation, all suggesting an upregulation of glycolytic capacity. Whilst the increase in hexokinase activity was not dependent on PPARα, occurring in mice of both genotypes, the increase in LDH dehydrogenase activity only occurred in wild-type mice, suggesting an unexpected influence of PPARα on *Ldh* expression. PPARβ/δ has been shown to decrease the expression ratio of *Ldha*/*Ldhb* in skeletal muscle (54), but we are not aware of any previously reported effects of PPARα. While *Ldhb* encodes a LDH isoform that encourages the conversion of lactate to pyruvate, the protein product of *Ldha* favours the conversion of pyruvate to lactate. It is plausible therefore, that PPARα ablation is compensated by an increase in PPARβ/δ, which prevents a hypoxia-induced increase in *Ldha*/*Ldhb*, though this would have to be confirmed with gene expression studies. Alternatively, PPARα is known to increase pyruvate dehydrogenase kinase (PDK)4 activity, leading to an attenuation of PDH activity. This could increase pyruvate concentration, which may feed forward to increase LDH activity. Indeed, whilst hypoxia increased PDH phosphorylation in wild-type mice, potentially via HIF-dependent upregulation of PDK1 (6, 7), this effect was blunted in *Ppara*$^{-/-}$ mice. Taken together, these data implicate a switch away from oxidative metabolism towards glycolysis in the hypoxic mouse heart.

Our data therefore suggest that PPARα plays a key role in regulating the process of metabolic remodelling that occurs in the hypoxic heart, and is essential for the effects of dietary nitrate in preserving oxidative metabolism. This is in contrast to our previous findings in skeletal muscle where the metabolic response to hypoxia +/- nitrate was found to be the same in wild-type mice and *Ppara*$^{-/-}$ mice (35). The difference between the two tissues, and greater dependence on PPARα in heart, might be explained by the higher expression of PPARα in cardiac muscle compared with skeletal muscle (3). Nitrate supplementation did exert effects in hypoxic skeletal muscle, but this may have been due to effects via PPARβ/δ (36), or through haemodynamic changes that alter blood flow and $O_2$ delivery (20). Our data do not definitively address whether nitrate exerts its effects by altering blood flow and therefore $O_2$ delivery or through direct effects on tissue metabolism. Although PPARα is an essential effector in this response, its transcriptional activity may simply be modified by HIF-signalling in response to changes in tissue oxygenation in order to ensure that oxidative metabolism is supported only when sufficient oxygen is available. Arguing against this is our finding here that hexokinase and LDH activity were increased by hypoxia in both chloride-supplemented and nitrate-supplemented hearts, indicating that whilst the dose of nitrate

employed here did modulate FAO, it was not sufficient to ameliorate the fall in oxygenation through improved blood flow. Moreover, our previous work in cultured myotubes indicated that nitrate enhanced PPARα activity without changes in oxygenation (34), and it would be interesting to replicate this in cardiomyocytes. It seems likely that nitrate exerts complementary but separate effects on blood flow and metabolism, ensuring that tissue $O_2$ supply and demand are matched.

Our work has implications for a number of conditions where cardiac and skeletal muscle metabolism is pathologically altered, particularly where derangements in NO production or availability have been implicated. For instance, endothelial NOS (eNOS) knockout mice develop a metabolic syndrome-like phenotype, including obesity and insulin resistance, yet features of the pathology were reversed following nitrate supplementation (55). It has been suggested that nitrate supplementation may be of benefit to patients with heart failure with reduced ejection fraction (HFrEF) in whom eNOS activity is impaired (56). A recent study demonstrated improvements in NO bioavailability and muscle power following nitrate supplementation in 9 patients with HFrEF (56) and it would be interesting to see if this was associated with changes in tissue metabolism in addition to improvements in blood flow. The failing heart itself is energy-starved (57) and characterised by a downregulation of FAO (1, 57), which may improve the efficiency of $O_2$ utilisation. It was shown, however, that oxygenation was not impaired in the non-ischaemic failing myocardium (58), and thus therapeutic strategies that enhance oxidative metabolism, including perhaps nitrate supplementation, may be of benefit to these patients.

In conclusion, hypoxia suppresses oxidative metabolism in the heart and enhances glycolytic capacity. In addition, there is a particular suppression of FAO in the hypoxic heart, which is mediated through decreased PPARα transcriptional activity, and can be reversed by supplementation with dietary nitrate in a PPARα-dependent manner.

**Acknowledgements**

This work was supported by the Biotechnology and Biological Sciences Research Council, UK [grant number: BB/F016581/1] and the Research Councils UK [grant number: EP/E500552/1]. The authors acknowledge the support of Professor Kieran Clarke (University of Oxford) and Professor Martin Feelisch (University of Southampton).

**Author Contributions**

JAH, KAO, SDRH and AJM designed research; JAH, KAO, ADC, RTL, ASS, NEKP and JD performed research; JAH, KAO, ADC, RTL, NEKP, MF and AJM analysed data; JAH, KAO, NEKP and AJM wrote the paper and all authors approved submission.

**References**


1. Lopaschuk, G. D., Ussher, J. R., Folmes, C. D., Jaswal, J. S., and Stanley, W. C. (2010) Myocardial fatty acid metabolism in health and disease. *Physiol Rev* **90**, 207-258
2. Essop, M. F. (2007) Cardiac metabolic adaptations in response to chronic hypoxia. *J Physiol* **584**, 715-726
3. Rakhshandehroo, M., Knoch, B., Muller, M., and Kersten, S. (2010) Peroxisome proliferator-activated receptor alpha target genes. *PPAR Res* **2010**
4. Wu, R., Chang, H. C., Khechaduri, A., Chawla, K., Tran, M., Chai, X., Wagg, C., Ghanefar, M., Jiang, X., Bayeva, M., Gonzalez, F., Lopaschuk, G., and Ardehali, H. (2014) Cardiac-specific ablation of ARNT leads to lipotoxicity and cardiomyopathy. *J Clin Invest* **124**, 4795-4806
5. Belanger, A. J., Luo, Z., Vincent, K. A., Akita, G. Y., Cheng, S. H., Gregory, R. J., and Jiang, C. (2007) Hypoxia-inducible factor 1 mediates hypoxia-induced cardiomyocyte lipid accumulation by reducing the DNA binding activity of peroxisome proliferator-activated receptor alpha/retinoid X receptor. *Biochem Biophys Res Commun* **364**, 567-572
6. Kim, J. W., Tchernyshyov, I., Semenza, G. L., and Dang, C. V. (2006) HIF-1-mediated expression of pyruvate dehydrogenase kinase: a metabolic switch required for cellular adaptation to hypoxia. *Cell Metab* **3**, 177-185
7. Papandreou, I., Cairns, R. A., Fontana, L., Lim, A. L., and Denko, N. C. (2006) HIF-1 mediates adaptation to hypoxia by actively downregulating mitochondrial oxygen consumption. *Cell Metab* **3**, 187-197
8. Cole, M. A., Abd Jamil, A. H., Heather, L. C., Murray, A. J., Sutton, E. R., Slingo, M., Sebag-Montefiore, L., Tan, S. C., Aksentijevic, D., Gildea, O. S., Stuckey, D. J., Yeoh, K. K., Carr, C. A., Evans, R. D., Aasum, E., Schofield, C. J., Ratcliffe, P. J., Neubauer, S., Robbins, P. A., and Clarke, K. (2016) On the pivotal role of PPARalpha in adaptation of the heart to hypoxia and why fat in the diet increases hypoxic injury. *FASEB J* **30**, 2684-2697
9. Horscroft, J. A., Burgess, S. L., Hu, Y., and Murray, A. J. (2015) Altered Oxygen Utilisation in Rat Left Ventricle and Soleus after 14 Days, but Not 2 Days, of Environmental Hypoxia. *PLoS One* **10**, e0138564
10. Holloway, C. J., Montgomery, H. E., Murray, A. J., Cochlin, L. E., Codreanu, I., Hopwood, N., Johnson, A. W., Rider, O. J., Levett, D. Z., Tyler, D. J., Francis, J. M.,

Neubauer, S., Grocott, M. P., Clarke, K., and Caudwell Xtreme Everest Research, G. (2011) Cardiac response to hypobaric hypoxia: persistent changes in cardiac mass, function, and energy metabolism after a trek to Mt. Everest Base Camp. *FASEB J* **25**, 792-796

11. Larsen, F. J., Schiffer, T. A., Borniquel, S., Sahlin, K., Ekblom, B., Lundberg, J. O., and Weitzberg, E. (2011) Dietary inorganic nitrate improves mitochondrial efficiency in humans. *Cell Metab* **13**, 149-159
12. Duncan, C., Dougall, H., Johnston, P., Green, S., Brogan, R., Leifert, C., Smith, L., Golden, M., and Benjamin, N. (1995) Chemical generation of nitric oxide in the mouth from the enterosalivary circulation of dietary nitrate. *Nat Med* **1**, 546-551
13. Benjamin, N., O'Driscoll, F., Dougall, H., Duncan, C., Smith, L., Golden, M., and McKenzie, H. (1994) Stomach NO synthesis. *Nature* **368**, 502
14. Shiva, S., Wang, X., Ringwood, L. A., Xu, X., Yuditskaya, S., Annavajjhala, V., Miyajima, H., Hogg, N., Harris, Z. L., and Gladwin, M. T. (2006) Ceruloplasmin is a NO oxidase and nitrite synthase that determines endocrine NO homeostasis. *Nat Chem Biol* **2**, 486-493
15. Gardner, P. R. (2005) Nitric oxide dioxygenase function and mechanism of flavohemoglobin, hemoglobin, myoglobin and their associated reductases. *J Inorg Biochem* **99**, 247-266
16. Millar, T. M., Stevens, C. R., Benjamin, N., Eisenthal, R., Harrison, R., and Blake, D. R. (1998) Xanthine oxidoreductase catalyses the reduction of nitrates and nitrite to nitric oxide under hypoxic conditions. *FEBS Lett* **427**, 225-228
17. Cosby, K., Partovi, K. S., Crawford, J. H., Patel, R. P., Reiter, C. D., Martyr, S., Yang, B. K., Waclawiw, M. A., Zalos, G., Xu, X., Huang, K. T., Shields, H., Kim-Shapiro, D. B., Schechter, A. N., Cannon, R. O., 3rd, and Gladwin, M. T. (2003) Nitrite reduction to nitric oxide by deoxyhemoglobin vasodilates the human circulation. *Nat Med* **9**, 1498-1505
18. Shiva, S., Huang, Z., Grubina, R., Sun, J., Ringwood, L. A., MacArthur, P. H., Xu, X., Murphy, E., Darley-Usmar, V. M., and Gladwin, M. T. (2007) Deoxymyoglobin is a nitrite reductase that generates nitric oxide and regulates mitochondrial respiration. *Circ Res* **100**, 654-661
19. Gautier, C., van Faassen, E., Mikula, I., Martasek, P., and Slama-Schwok, A. (2006) Endothelial nitric oxide synthase reduces nitrite anions to NO under anoxia. *Biochem Biophys Res Commun* **341**, 816-821

20. Palmer, R. M., Ferrige, A. G., and Moncada, S. (1987) Nitric oxide release accounts for the biological activity of endothelium-derived relaxing factor. *Nature* **327**, 524-526
21. Mittal, C. K., and Murad, F. (1977) Properties and oxidative regulation of guanylate cyclase. *J Cyclic Nucleotide Res* **3**, 381-391
22. Taylor, D. A., Bowman, B. F., and Stull, J. T. (1989) Cytoplasmic Ca2+ is a primary determinant for myosin phosphorylation in smooth muscle cells. *J Biol Chem* **264**, 6207-6213
23. Ashmore, T., Fernandez, B. O., Evans, C. E., Huang, Y., Branco-Price, C., Griffin, J. L., Johnson, R. S., Feelisch, M., and Murray, A. J. (2015) Suppression of erythropoiesis by dietary nitrate. *FASEB J* **29**, 1102-1112
24. Martin, D. S., Ince, C., Goedhart, P., Levett, D. Z., Grocott, M. P., and Caudwell Xtreme Everest Research, G. (2009) Abnormal blood flow in the sublingual microcirculation at high altitude. *Eur J Appl Physiol* **106**, 473-478
25. Erzurum, S. C., Ghosh, S., Janocha, A. J., Xu, W., Bauer, S., Bryan, N. S., Tejero, J., Hemann, C., Hille, R., Stuehr, D. J., Feelisch, M., and Beall, C. M. (2007) Higher blood flow and circulating NO products offset high-altitude hypoxia among Tibetans. *Proc Natl Acad Sci U S A* **104**, 17593-17598
26. Beall, C. M., Cavalleri, G. L., Deng, L., Elston, R. C., Gao, Y., Knight, J., Li, C., Li, J. C., Liang, Y., McCormack, M., Montgomery, H. E., Pan, H., Robbins, P. A., Shianna, K. V., Tam, S. C., Tsering, N., Veeramah, K. R., Wang, W., Wangdui, P., Weale, M. E., Xu, Y., Xu, Z., Yang, L., Zaman, M. J., Zeng, C., Zhang, L., Zhang, X., Zhaxi, P., and Zheng, Y. T. (2010) Natural selection on EPAS1 (HIF2alpha) associated with low hemoglobin concentration in Tibetan highlanders. *Proc Natl Acad Sci U S A* **107**, 11459-11464
27. Nisoli, E., Tonello, C., Cardile, A., Cozzi, V., Bracale, R., Tedesco, L., Falcone, S., Valerio, A., Cantoni, O., Clementi, E., Moncada, S., and Carruba, M. O. (2005) Calorie restriction promotes mitochondrial biogenesis by inducing the expression of eNOS. *Science* **310**, 314-317
28. Brown, G. C., and Cooper, C. E. (1994) Nanomolar concentrations of nitric oxide reversibly inhibit synaptosomal respiration by competing with oxygen at cytochrome oxidase. *FEBS Lett* **356**, 295-298
29. Huie, R. E., and Padmaja, S. (1993) The reaction of no with superoxide. *Free Radic Res Commun* **18**, 195-199

30. Radi, R. (2013) Peroxynitrite, a stealthy biological oxidant. *J Biol Chem* **288**, 26464-26472
31. Clementi, E., Brown, G. C., Feelisch, M., and Moncada, S. (1998) Persistent inhibition of cell respiration by nitric oxide: crucial role of S-nitrosylation of mitochondrial complex I and protective action of glutathione. *Proc Natl Acad Sci U S A* **95**, 7631-7636
32. Larsen, F. J., Weitzberg, E., Lundberg, J. O., and Ekblom, B. (2010) Dietary nitrate reduces maximal oxygen consumption while maintaining work performance in maximal exercise. *Free Radic Biol Med* **48**, 342-347
33. Ashmore, T., Fernandez, B. O., Branco-Price, C., West, J. A., Cowburn, A. S., Heather, L. C., Griffin, J. L., Johnson, R. S., Feelisch, M., and Murray, A. J. (2014) Dietary nitrate increases arginine availability and protects mitochondrial complex I and energetics in the hypoxic rat heart. *J Physiol* **592**, 4715-4731
34. Ashmore, T., Roberts, L. D., Morash, A. J., Kotwica, A. O., Finnerty, J., West, J. A., Murfitt, S. A., Fernandez, B. O., Branco, C., Cowburn, A. S., Clarke, K., Johnson, R. S., Feelisch, M., Griffin, J. L., and Murray, A. J. (2015) Nitrate enhances skeletal muscle fatty acid oxidation via a nitric oxide-cGMP-PPAR-mediated mechanism. *BMC Biol* **13**, 110
35. O'Brien, K. A., Horscroft, J. A., Devaux, J., Lindsay, R. T., Steel, A. S., Clark, A. D., Philp, A., Harridge, S. D. R., and Murray, A. J. (2018) PPARalpha-independent effects of nitrate supplementation on skeletal muscle metabolism in hypoxia. *Biochim Biophys Acta Mol Basis Dis*
36. Muoio, D. M., MacLean, P. S., Lang, D. B., Li, S., Houmard, J. A., Way, J. M., Winegar, D. A., Corton, J. C., Dohm, G. L., and Kraus, W. E. (2002) Fatty acid homeostasis and induction of lipid regulatory genes in skeletal muscles of peroxisome proliferator-activated receptor (PPAR) alpha knock-out mice. Evidence for compensatory regulation by PPAR delta. *J Biol Chem* **277**, 26089-26097
37. Pesta, D., and Gnaiger, E. (2012) High-resolution respirometry: OXPHOS protocols for human cells and permeabilized fibers from small biopsies of human muscle. *Methods Mol Biol* **810**, 25-58
38. Heather, L. C., Cole, M. A., Tan, J. J., Ambrose, L. J., Pope, S., Abd-Jamil, A. H., Carter, E. E., Dodd, M. S., Yeoh, K. K., Schofield, C. J., and Clarke, K. (2012) Metabolic adaptation to chronic hypoxia in cardiac mitochondria. *Basic Res Cardiol* **107**, 268

39. Horscroft, J. A., Kotwica, A. O., Laner, V., West, J. A., Hennis, P. J., Levett, D. Z. H., Howard, D. J., Fernandez, B. O., Burgess, S. L., Ament, Z., Gilbert-Kawai, E. T., Vercueil, A., Landis, B. D., Mitchell, K., Mythen, M. G., Branco, C., Johnson, R. S., Feelisch, M., Montgomery, H. E., Griffin, J. L., Grocott, M. P. W., Gnaiger, E., Martin, D. S., and Murray, A. J. (2017) Metabolic basis to Sherpa altitude adaptation. *Proc Natl Acad Sci U S A* **114**, 6382-6387
40. Houle-Leroy, P., Garland, T., Jr., Swallow, J. G., and Guderley, H. (2000) Effects of voluntary activity and genetic selection on muscle metabolic capacities in house mice Mus domesticus. *J Appl Physiol (1985)* **89**, 1608-1616
41. McClelland, G. B., Dalziel, A. C., Fragoso, N. M., and Moyes, C. D. (2005) Muscle remodeling in relation to blood supply: implications for seasonal changes in mitochondrial enzymes. *J Exp Biol* **208**, 515-522
42. Levett, D. Z., Radford, E. J., Menassa, D. A., Graber, E. F., Morash, A. J., Hoppeler, H., Clarke, K., Martin, D. S., Ferguson-Smith, A. C., Montgomery, H. E., Grocott, M. P., Murray, A. J., and Caudwell Xtreme Everest Research Group. (2012) Acclimatization of skeletal muscle mitochondria to high-altitude hypoxia during an ascent of Everest. *FASEB J* **26**, 1431-1441
43. Cohen, B. H. (2013) *Explaining psychological statistics*, Wiley, Hoboken, New Jersey
44. Larsen, S., Nielsen, J., Hansen, C. N., Nielsen, L. B., Wibrand, F., Stride, N., Schroder, H. D., Boushel, R., Helge, J. W., Dela, F., and Hey-Mogensen, M. (2012) Biomarkers of mitochondrial content in skeletal muscle of healthy young human subjects. *J Physiol* **590**, 3349-3360
45. Palmer, J. W., Tandler, B., and Hoppel, C. L. (1985) Biochemical differences between subsarcolemmal and interfibrillar mitochondria from rat cardiac muscle: effects of procedural manipulations. *Arch Biochem Biophys* **236**, 691-702
46. Siervo, M., Stephan, B. C., Feelisch, M., and Bluck, L. J. (2011) Measurement of in vivo nitric oxide synthesis in humans using stable isotopic methods: a systematic review. *Free Radic Biol Med* **51**, 795-804
47. Pannala, A. S., Mani, A. R., Spencer, J. P., Skinner, V., Bruckdorfer, K. R., Moore, K. P., and Rice-Evans, C. A. (2003) The effect of dietary nitrate on salivary, plasma, and urinary nitrate metabolism in humans. *Free Radic Biol Med* **34**, 576-584
48. Velmurugan, S., Kapil, V., Ghosh, S. M., Davies, S., McKnight, A., Aboud, Z., Khambata, R. S., Webb, A. J., Poole, A., and Ahluwalia, A. (2013) Antiplatelet

effects of dietary nitrate in healthy volunteers: involvement of cGMP and influence of sex. *Free Radic Biol Med* **65**, 1521-1532

49. Roberts, L. D., Ashmore, T., Kotwica, A. O., Murfitt, S. A., Fernandez, B. O., Feelisch, M., Murray, A. J., and Griffin, J. L. (2015) Inorganic nitrate promotes the browning of white adipose tissue through the nitrate-nitrite-nitric oxide pathway. *Diabetes* **64**, 471-484
50. Roberts, L. D., Ashmore, T., McNally, B. D., Murfitt, S. A., Fernandez, B. O., Feelisch, M., Lindsay, R., Siervo, M., Williams, E. A., Murray, A. J., and Griffin, J. L. (2017) Inorganic Nitrate Mimics Exercise-Stimulated Muscular Fiber-Type Switching and Myokine and gamma-Aminobutyric Acid Release. *Diabetes* **66**, 674-688
51. Hezel, M. P., Liu, M., Schiffer, T. A., Larsen, F. J., Checa, A., Wheelock, C. E., Carlstrom, M., Lundberg, J. O., and Weitzberg, E. (2015) Effects of long-term dietary nitrate supplementation in mice. *Redox Biol* **5**, 234-242
52. Selmeci, L., Farkas, A., Posch, E., Szelenyi, I., and Sos, J. (1967) The effect of hypoxia on the lactic dehydrogenase (LDH) activity of serum and heart muscle of rats. *Life Sci* **6**, 649-653
53. Horscroft, J. A., and Murray, A. J. (2014) Skeletal muscle energy metabolism in environmental hypoxia: climbing towards consensus. *Extrem Physiol Med* **3**, 19
54. Gan, Z., Burkart-Hartman, E. M., Han, D.-H., Finck, B., Leone, T. C., Smith, E. Y., Ayala, J. E., Holloszy, J., and Kelly, D. P. (2011) The nuclear receptor PPARβ/δ programs muscle glucose metabolism in cooperation with AMPK and MEF2. *Genes & development* **25**, 2619-2630
55. Carlstrom, M., Larsen, F. J., Nystrom, T., Hezel, M., Borniquel, S., Weitzberg, E., and Lundberg, J. O. (2010) Dietary inorganic nitrate reverses features of metabolic syndrome in endothelial nitric oxide synthase-deficient mice. *Proc Natl Acad Sci U S A* **107**, 17716-17720
56. Mulkareddy, V., Racette, S. B., Coggan, A. R., and Peterson, L. R. (2018) Dietary nitrate's effects on exercise performance in heart failure with reduced ejection fraction (HFrEF). *Biochim Biophys Acta Mol Basis Dis*
57. Neubauer, S. (2007) The failing heart--an engine out of fuel. *N Engl J Med* **356**, 1140-1151
58. Dass, S., Holloway, C. J., Cochlin, L. E., Rider, O. J., Mahmod, M., Robson, M., Sever, E., Clarke, K., Watkins, H., Ashrafian, H., Karamitsos, T. D., and Neubauer, S.

(2015) No Evidence of Myocardial Oxygen Deprivation in Nonischemic Heart Failure. *Circ Heart Fail* **8**, 1088-1093

## Figure Legends

**Figure 1** **Study design.** Each stage of the study took place within the ages shown ± 4 d, and the length of each stage was identical for each mouse. The left-hand section represents wild-type (*Ppara*$^{+/+}$) mice, whilst the right-hand section represents *Ppara*$^{-/-}$ mice. The number in brackets indicates the number of mice per group. Chloride, 0.7 mM NaCl in distilled water *ad libitum*; Nitrate, 0.7 mM $NaNO_3$ in distilled water *ad libitum*; Normoxia, 21% atmospheric $O_2$; Hypoxia, 10% atmospheric $O_2$. Background patterns reflect those used in figures throughout this manuscript.

**Figure 2** **Mitochondrial respiratory function from Assay 1 normalised to mass.** A) Malate and palmitoyl CoA stimulated LEAK respiration ($CPT1_L$); B) CPT1-limited OXPHOS ($CPT1_P$); C) OXPHOS supported by the F-pathway via β-oxidation ($PalM_P$) in permeabilised cardiac muscle fibres from wild-type (*Ppara*$^{+/+}$) and *Ppara*$^{-/-}$ mice following normoxia (white bars, 21% $O_2$) or hypoxia (blue bars, 10% $O_2$), and chloride (open bars, 0.7 mM NaCl) or nitrate (striped bars, 0.7 mM $NaNO_3$) supplementation. Error bars indicate SEM. * = main effect. Blue symbols (*) = hypoxia effect; black symbols (*) = PPARα effect. 1 symbol (*) = $P < 0.05$; 2 symbols (**) = $P < 0.01$; 3 symbols (***) = $P < 0.001$. Symbols in brackets (e.g. (*)) denote significance of a test of a combination of groups (i.e. main effects or two-way interactions) as described in the text. $n$ = 8-11 per group.

**Figure 3** **Mitochondrial respiratory function from Assay 2 normalised to mass.** A) Malate and octanoyl carnitine stimulated LEAK respiration ($OctM_L$); B) OXPHOS supported by the F-pathway via β-oxidation ($OctM_P$); C) OXPHOS supported by pyruvate and malate through the N-pathway via complex I ($PM_P$); D) OXPHOS supported by glutamate and malate through the N-pathway via complex I ($GM_P$); E) OXPHOS supported by glutamate, malate and succinate through the NS-pathway via complexes I and II ($GMS_P$); F) by succinate following the addition of rotenone ($S_P$) in permeabilised cardiac muscle fibres from wild-type (*Ppara*$^{+/+}$) and *Ppara*$^{-/-}$ mice following normoxia (white bars, 21% $O_2$) or hypoxia (blue bars, 10% $O_2$), and chloride (open bars, 0.7 mM NaCl) or nitrate (striped bars, 0.7 mM $NaNO_3$) supplementation.

Error bars indicate SEM. * = main effect. Blue symbols (*) = hypoxia effect; black symbols (*) = PPARα effect. 1 symbol (*) = $P < 0.05$; 2 symbols (**) = $P < 0.01$; 3 symbols (***) = $P < 0.001$. Symbols in brackets (e.g. $^{(**)}$) denote significance of a test of a combination of groups (i.e. main effects or two-way interactions) as described in the text. $n$ = 8-11 per group.

**Figure 4** **Mitochondrial respiratory function from Assay 1 normalised to citrate synthase activity.** A) Malate and palmitoyl CoA stimulated LEAK respiration ($CPT1_L$); B) CPT1-limited OXPHOS ($CPT1_P$); C) OXPHOS supported by the F-pathway via β-oxidation ($PalM_P$) in permeabilised cardiac muscle fibres from wild-type ($Ppara^{+/+}$) and $Ppara^{-/-}$ mice following normoxia (white bars, 21% $O_2$) or hypoxia (blue bars, 10% $O_2$), and chloride (open bars, 0.7 mM NaCl) or nitrate (striped bars, 0.7 mM $NaNO_3$) supplementation. Error bars indicate SEM. $^{\Delta}$ = two-way interaction. Orange symbols ($^{\Delta}$) = nitrate effect; black symbols ($^{\Delta}$) = PPARα effect. 1 symbol ($^{\Delta}$) = $P < 0.05$; 2 symbols ($^{\Delta\Delta}$) = $P < 0.01$; 3 symbols ($^{\Delta\Delta\Delta}$) = $P < 0.001$. Symbols in brackets (e.g. $^{(\Delta)}$) denote significance of a test of a combination of groups (i.e. main effects or two-way interactions) as described in the text. $n$ = 4-6 per group.

**Figure 5** **Mitochondrial respiratory function from Assay 2 normalised to citrate synthase activity.** A) Malate and octanoyl carnitine stimulated LEAK respiration ($OctM_L$); B) OXPHOS supported by the F-pathway via β-oxidation ($OctM_P$); C) OXPHOS supported by pyruvate and malate through the N-pathway via complex I ($PM_P$); D) OXPHOS supported by glutamate and malate through the N-pathway via complex I ($GM_P$); E) OXPHOS supported by glutamate, malate and succinate through the NS-pathway via complexes I and II ($GMS_P$); F) OXPHOS supported by by succinate following the addition of rotenone ($S_P$) in permeabilised cardiac muscle fibres from wild-type ($Ppara^{+/+}$) and $Ppara^{-/-}$ mice following normoxia (white bars, 21% $O_2$) or hypoxia (blue bars, 10% $O_2$), and chloride (open bars, 0.7 mM NaCl) or nitrate (striped bars, 0.7 mM $NaNO_3$) supplementation. Error bars indicate SEM. Black symbols (*) = PPARα effect. 1 symbol (*) = $P < 0.05$; 2 symbols (**) = $P < 0.01$; 3 symbols (***) = $P < 0.001$. $n$ = 4-6 per group.

**Figure 6** **Substrate control ratios.** Ratios indicate A) CPT1 control over β-oxidation ($FCR_{CPT1}$); B) the contribution of the F-pathway via β-oxidation to maximal OXPHOS ($FCR_F$) and C) the capacity for OXPHOS supported by octanoyl carnitine plus malate relative to pyruvate plus malate ($FCR_{Oct/P}$), in permeabilised cardiac muscle fibres from wild-type (*Ppara*$^{+/+}$) and *Ppara*$^{-/-}$ mice, following normoxia (white bars, 21% $O_2$) or hypoxia (blue bars, 10% $O_2$), and chloride (open bars, 0.7 mM NaCl) or nitrate (striped bars, 0.7 mM $NaNO_3$) supplementation. Error bars indicate SEM. $^{\Delta}$ = two-way interaction; † = three-way interaction. Orange symbols ($^{\dagger}$) = nitrate effect; blue symbols ($^{\Delta}$, $^{\dagger}$) = hypoxia effect; black symbols ($^{\Delta}$, $^{\dagger}$) = PPARα effect. 1 symbol ($^{\dagger}$) = $P$ < 0.05; 3 symbols ($^{\Delta\Delta\Delta}$, $^{\dagger\dagger\dagger}$) = $P$ < 0.001. $n$ = 8-10 per group.

**Figure 7** **Enzyme activities in mouse heart tissue homogenates.** Maximal activity of A) citrate synthase (CS); B) 3-hydroxyacyl dehydrogenase (HADH); C) hexokinase (HK) and D) lactate dehydrogenase (LDH) from wild-type (*Ppara*$^{+/+}$) and *Ppara*$^{-/-}$ mice, following normoxia (white bars, 21% $O_2$) or hypoxia (blue bars, 10% $O_2$), and chloride (open bars, 0.7 mM NaCl) or nitrate (striped bars, 0.7 mM $NaNO_3$) supplementation. Error bars indicate SEM. *** $P$ < 0.001, hypoxia main effect; $^{\Delta\Delta}$ $P$ < 0.01, nitrate effect following nitrate/PPARα interaction; $^{\Delta\Delta\Delta}$ $P$ < 0.001, hypoxia effect following hypoxia/PPARα interaction; $^{\Delta\Delta}$ $P$ < 0.01, PPARα effect following nitrate/PPARα interaction; $^{\Delta\Delta\Delta}$ $P$ < 0.01, PPARα effect following hypoxia/PPARα interaction. Symbols in brackets denote significance of a test of a combination of groups (i.e. main effects or two-way interactions) as described in the text. $n$ = 4-5 per group.

**Figure 8** **Total pyruvate dehydrogenase (PDH) levels and phosphorylation.** Protein levels of A) total PDH; and phosphorylation of PDH at E1α site B) serine 232 (pPDH S232); C) serine 293 (pPDH S293) and D) serine 300 (pPDH S300) in wild-type (*Ppara*$^{+/+}$) and *Ppara*$^{-/-}$ mice, following normoxia (white bars, 21% $O_2$) or hypoxia (blue bars, 10% $O_2$), and chloride (open bars, 0.7 mM NaCl) or nitrate (striped bars, 0.7 mM $NaNO_3$) supplementation. Error bars indicate SEM. $^{\Delta}$ = two-way interaction; † = three-way interaction. Blue symbols ($^{\Delta}$, $^{\dagger}$) = hypoxia effect; black symbols ($^{\dagger}$) = PPARα effect. 1 symbol ($^{\dagger}$) = $P$ < 0.05; 2 symbols ($^{\Delta\Delta}$, $^{\dagger\dagger}$) = $P$ < 0.05 3 symbols ($^{\dagger\dagger\dagger}$) = $P$ < 0.001. $n$ = 8-10 per group.

# Figure 1

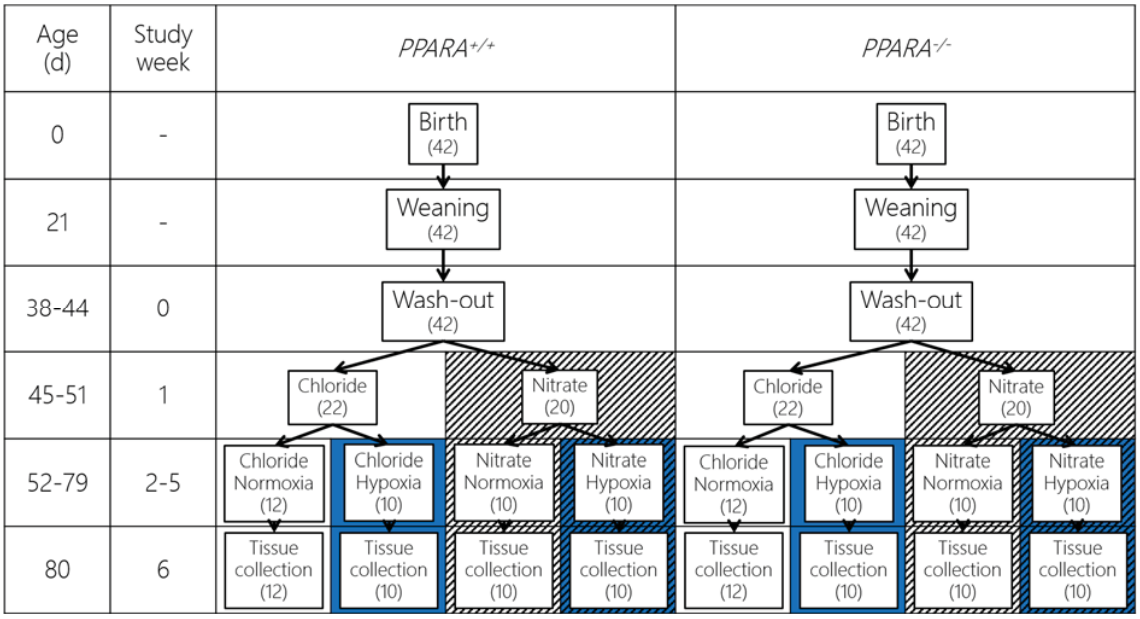
Age (d)
Study week
PPARA+/+
PPARA-/-
0
-
Birth (42)
21
-
Weaning (42)
38-44
0
Wash-out (42)
45-51
1
Chloride (22)
Nitrate (20)
52-79
2-5
Chloride Normoxia (12)
Chloride Hypoxia (10)
Nitrate Normoxia (10)
Nitrate Hypoxia (10)
80
6
Tissue collection (12)
Tissue collection (10)
Tissue collection (10)
Tissue collection (10)

# Figure 2

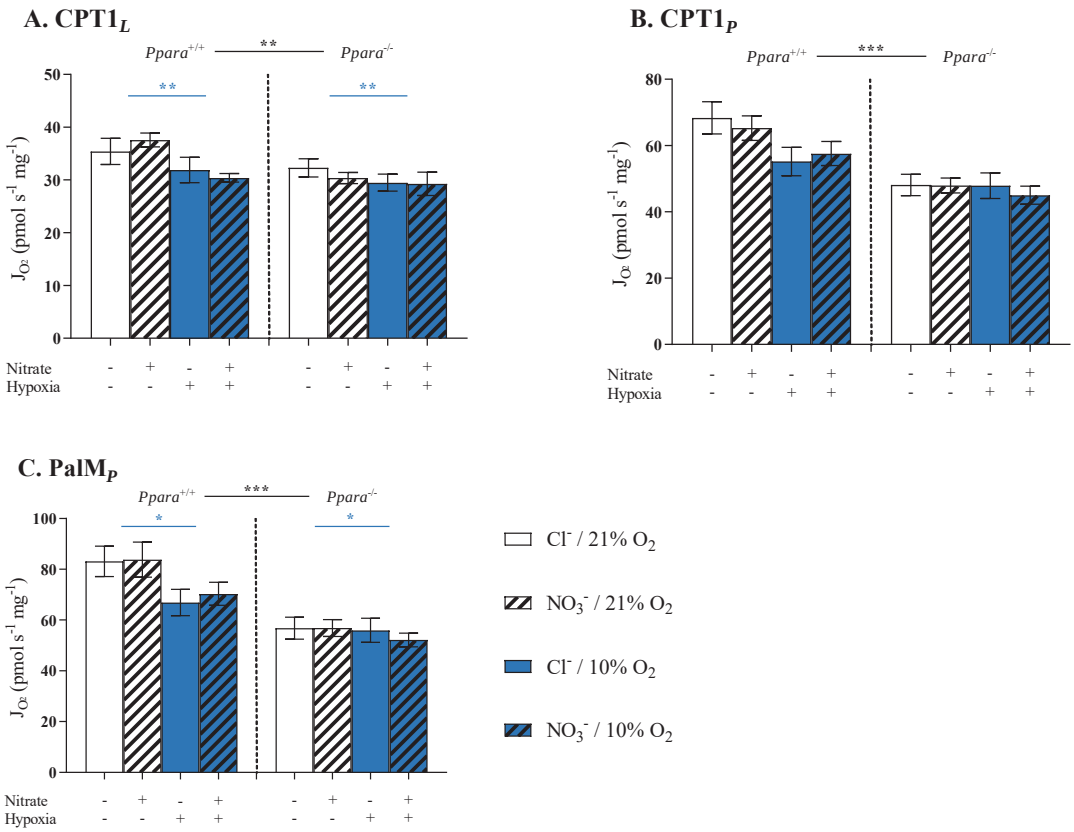
A. CPT1$_L$
Ppara$^{+/+}$
**
Ppara$^{-/-}$
**
**
$J_{O_2}$ (pmol s$^{-1}$ mg$^{-1}$)
50
40
30
20
10
0
Nitrate - + - + - + - +
Hypoxia - - + + - - + +
B. CPT1$_P$
Ppara$^{+/+}$
***
Ppara$^{-/-}$
$J_{O_2}$ (pmol s$^{-1}$ mg$^{-1}$)
80
60
40
20
0
Nitrate - + - + - + - +
Hypoxia - - + + - - + +
C. PalM$_P$
Ppara$^{+/+}$
***
Ppara$^{-/-}$
*
*
$J_{O_2}$ (pmol s$^{-1}$ mg$^{-1}$)
100
80
60
40
20
0
Nitrate - + - + - + - +
Hypoxia - - + + - - + +
Cl$^-$ / 21% $O_2$
$NO_3^-$ / 21% $O_2$
Cl$^-$ / 10% $O_2$
$NO_3^-$ / 10% $O_2$

# Figure 3

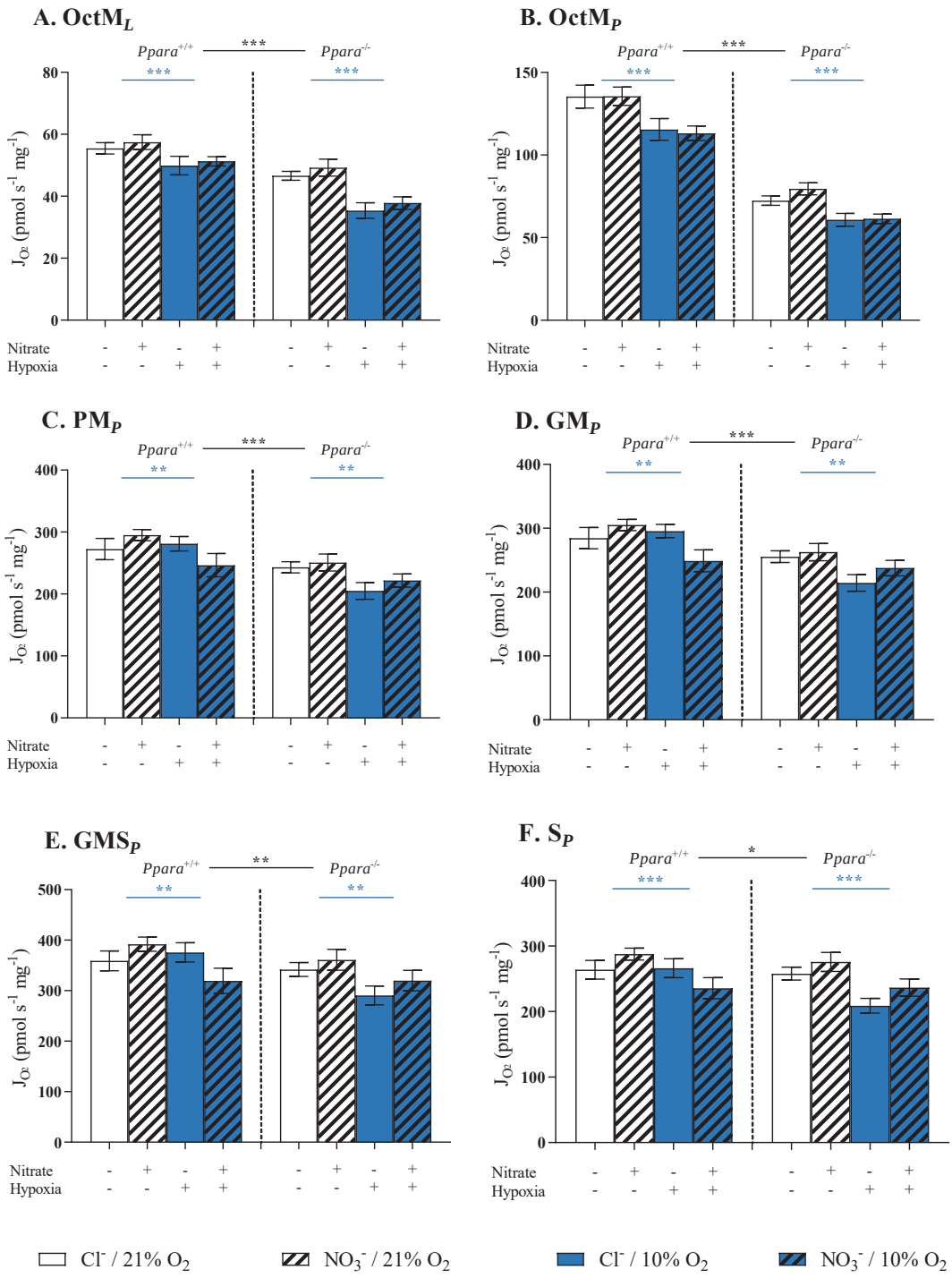
A. OctM$_L$
B. OctM$_P$
C. PM$_P$
D. GM$_P$
E. GMS$_P$
F. S$_P$
Ppara$^{+/+}$
Ppara$^{-/-}$
$J_{O_2}$ (pmol s$^{-1}$ mg$^{-1}$)
Nitrate
Hypoxia
Cl$^-$ / 21% O$_2$
NO$_3^-$ / 21% O$_2$
Cl$^-$ / 10% O$_2$
NO$_3^-$ / 10% O$_2$

# Figure 4

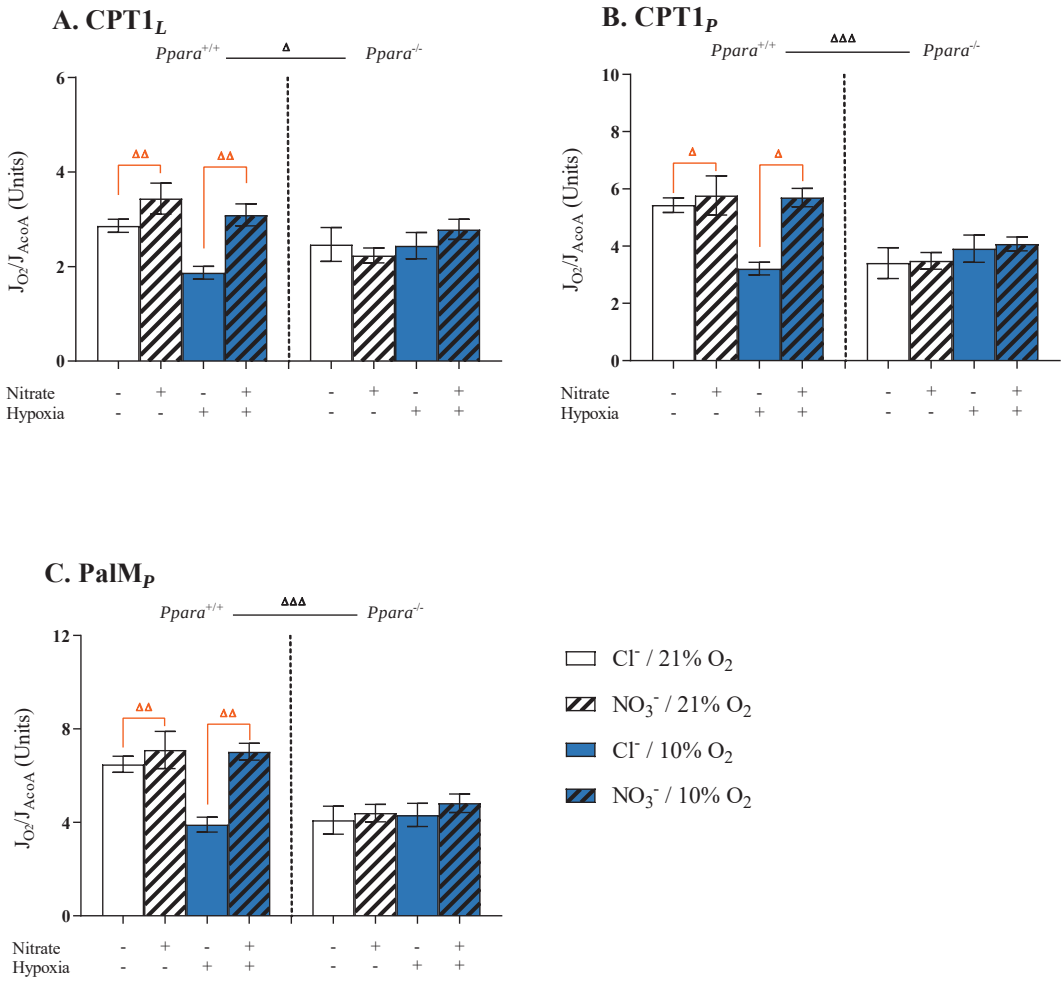
A. CPT1L
Ppara+/+
Ppara-/-
JO2/JAcoA (Units)
Nitrate
Hypoxia
B. CPT1P
C. PalMP
Cl- / 21% O2
NO3- / 21% O2
Cl- / 10% O2
NO3- / 10% O2

# Figure 5

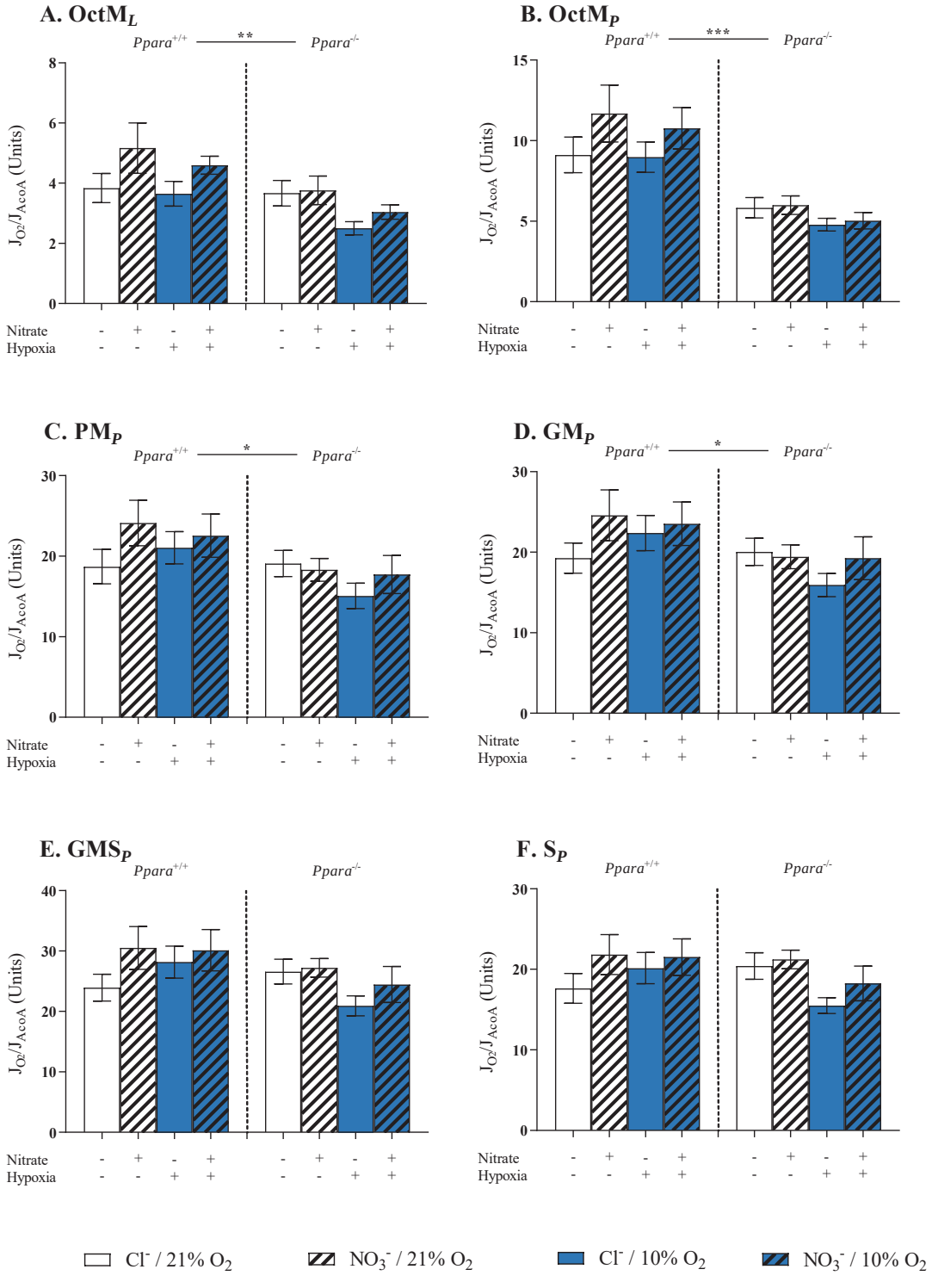
A. OctM$_L$
B. OctM$_P$
C. PM$_P$
D. GM$_P$
E. GMS$_P$
F. S$_P$
Ppara$^{+/+}$
Ppara$^{-/-}$
**
***
*
$J_{O2}/J_{AcoA}$ (Units)
Nitrate
Hypoxia
Cl$^-$ / 21% O$_2$
NO$_3^-$ / 21% O$_2$
Cl$^-$ / 10% O$_2$
NO$_3^-$ / 10% O$_2$

# Figure 6

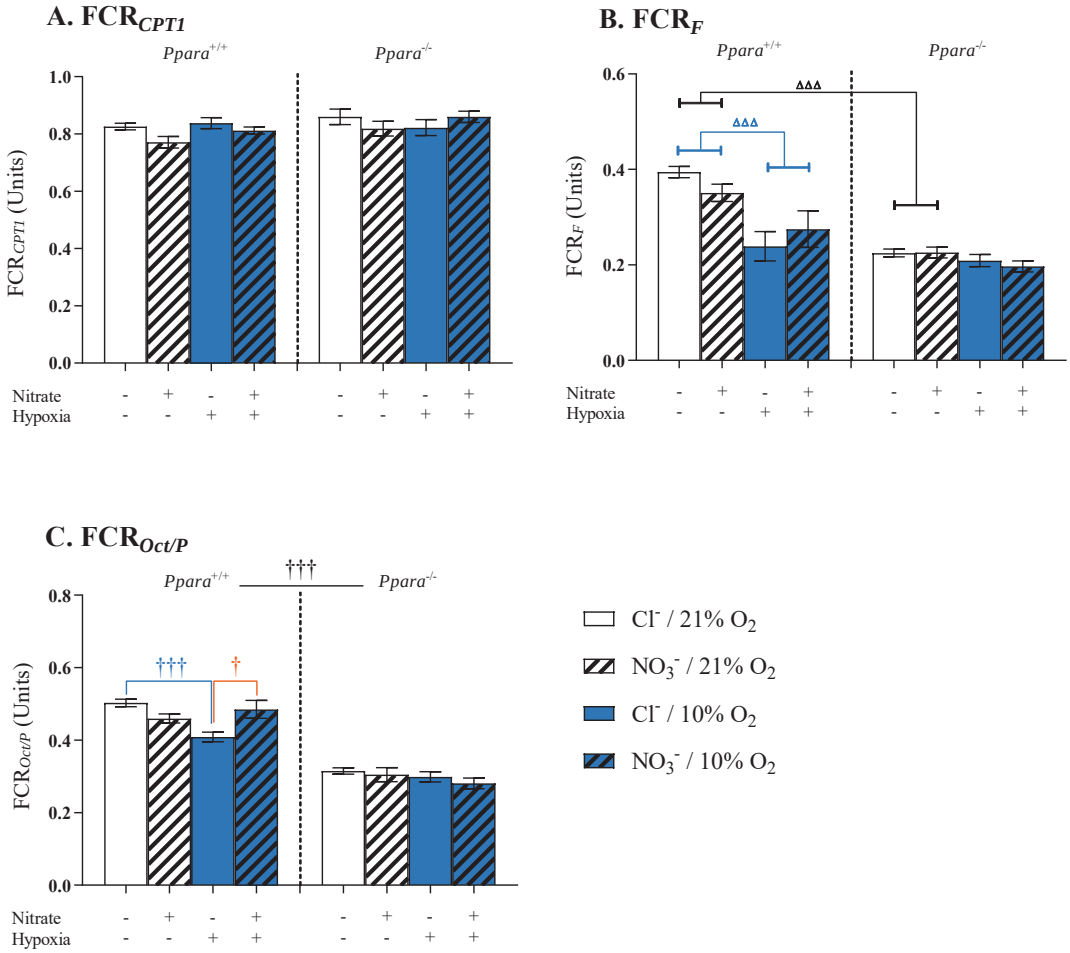
A. FCR$_{CPT1}$
Ppara$^{+/+}$
Ppara$^{-/-}$
FCR$_{CPT1}$ (Units)
1.0
0.8
0.6
0.4
0.2
0.0
Nitrate - + - + - + - +
Hypoxia - - + + - - + +
B. FCR$_F$
Ppara$^{+/+}$
Ppara$^{-/-}$
ΔΔΔ
ΔΔΔ
FCR$_F$ (Units)
0.6
0.4
0.2
0.0
Nitrate - + - + - + - +
Hypoxia - - + + - - + +
C. FCR$_{Oct/P}$
Ppara$^{+/+}$
Ppara$^{-/-}$
†††
†††
†
FCR$_{Oct/P}$ (Units)
0.8
0.6
0.4
0.2
0.0
Nitrate - + - + - + - +
Hypoxia - - + + - - + +
Cl$^-$ / 21% O$_2$
NO$_3^-$ / 21% O$_2$
Cl$^-$ / 10% O$_2$
NO$_3^-$ / 10% O$_2$

# Figure 7

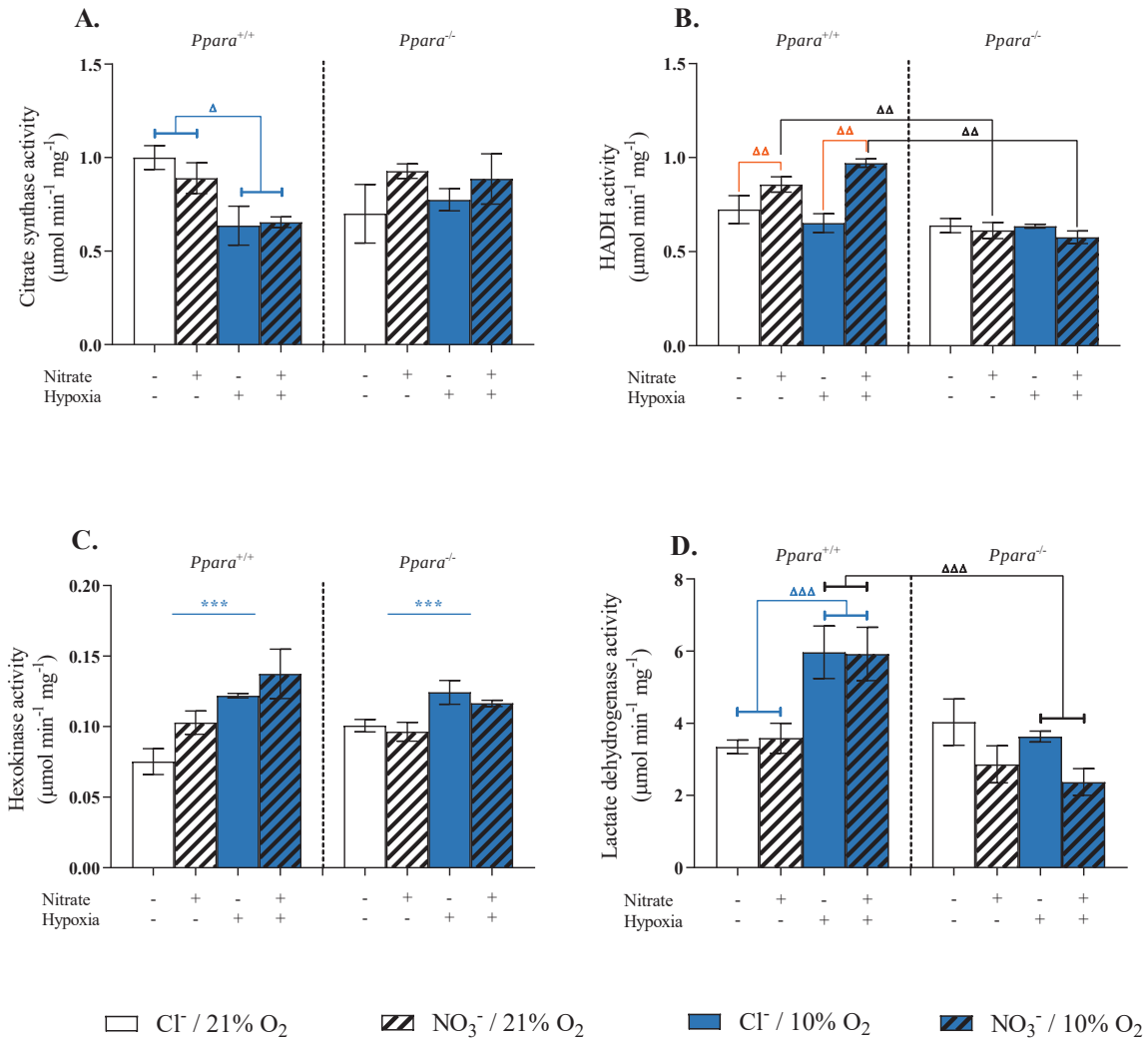
A.
Ppara+/+
Ppara-/-
Citrate synthase activity (µmol min-1 mg-1)
1.5
1.0
0.5
0.0
Δ
Nitrate - + - + - + - +
Hypoxia - - + + - - + +
B.
Ppara+/+
Ppara-/-
HADH activity (µmol min-1 mg-1)
1.5
1.0
0.5
0.0
ΔΔ
ΔΔ
ΔΔ
Nitrate - + - + - + - +
Hypoxia - - + + - - + +
C.
Ppara+/+
Ppara-/-
Hexokinase activity (µmol min-1 mg-1)
0.20
0.15
0.10
0.05
0.00
***
***
Nitrate - + - + - + - +
Hypoxia - - + + - - + +
D.
Ppara+/+
Ppara-/-
Lactate dehydrogenase activity (µmol min-1 mg-1)
8
6
4
2
0
ΔΔΔ
ΔΔΔ
Nitrate - + - + - + - +
Hypoxia - - + + - - + +
Cl- / 21% O2
NO3- / 21% O2
Cl- / 10% O2
NO3- / 10% O2

# Figure 8

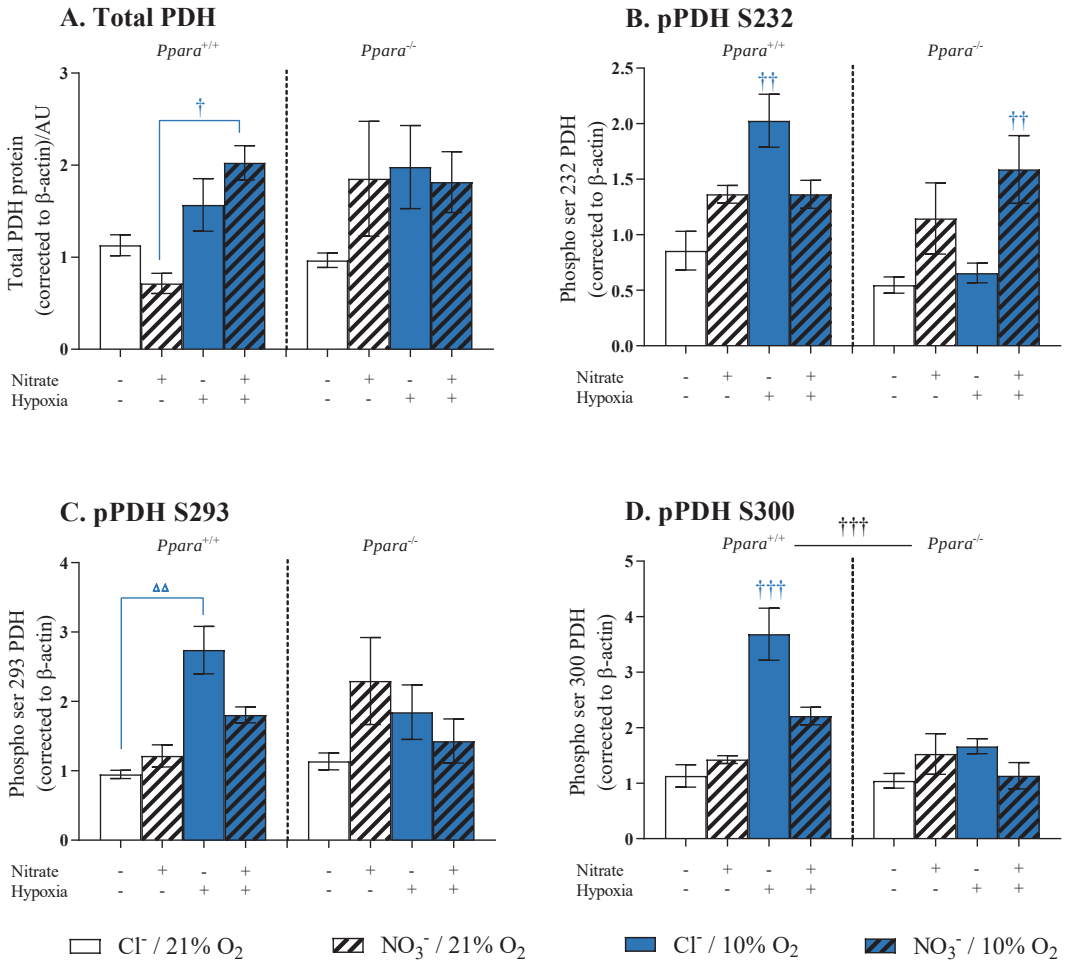
A. Total PDH
Ppara+/+
Ppara-/-
Total PDH protein (corrected to β-actin)/AU
†
Nitrate
Hypoxia
B. pPDH S232
Phospho ser 232 PDH (corrected to β-actin)
††
C. pPDH S293
Phospho ser 293 PDH (corrected to β-actin)
ΔΔ
D. pPDH S300
Phospho ser 300 PDH (corrected to β-actin)
†††
Cl- / 21% O2
NO3- / 21% O2
Cl- / 10% O2
NO3- / 10% O2

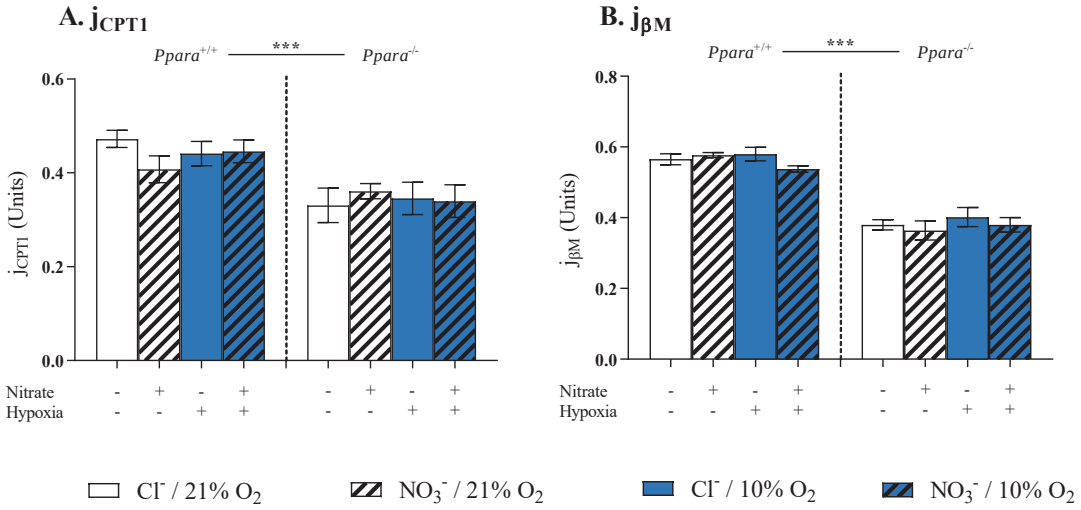


**Supplementary Figure 1: OXPHOS coupling efficiencies (j)**

A) From Assay 1 ($j_{CPT1}$) and B) Assay 2 ($j_{OctM}$) in permeabilised cardiac fibres from wild-type (*Ppara*$^{+/+}$) and *Ppara*$^{-/-}$ mice, following normoxia (white bars, 21% $O_2$) or hypoxia (blue bars, 10% $O_2$), and chloride (open bars, 0.7 mM NaCl) or nitrate (striped bars, 0.7 mM $NaNO_3$) supplementation. Error bars indicate SEM. *** = PPARα main effect at $P < 0.001$. $n$ = 8-10 per group.

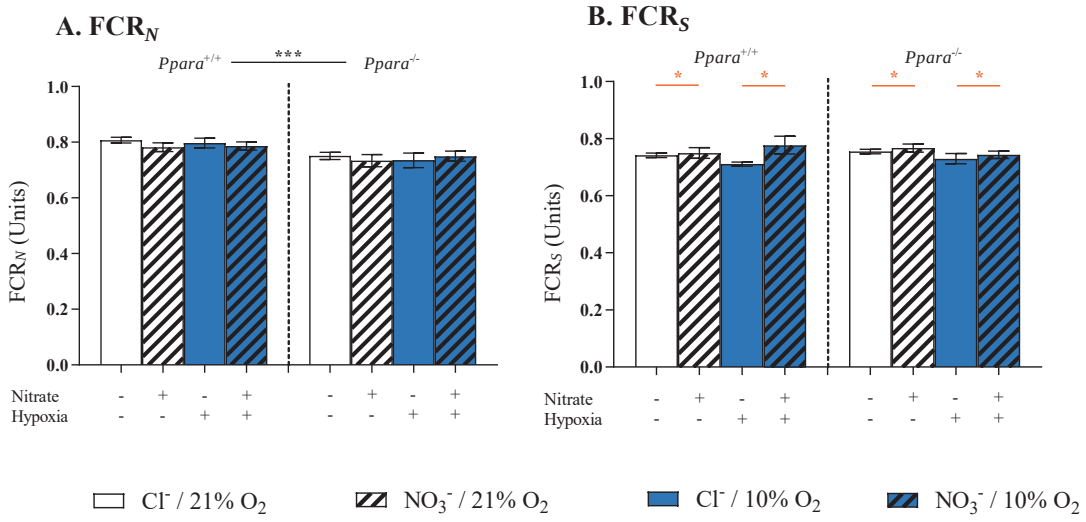


**Supplementary Figure 2: Substrate control ratios**

Ratios indicate the contributions of A) the N-pathway via complex I to maximal OXPHOS ($FCR_N$) and B) the S-pathway via complex II to maximal OXPHOS ($FCR_S$) in permeabilised cardiac muscle fibres from wild-type (*Ppara*$^{+/+}$) and *Ppara*$^{-/-}$ mice, following normoxia (white bars, 21% $O_2$) or hypoxia (blue bars, 10% $O_2$), and chloride (open bars, 0.7 mM NaCl) or nitrate (striped bars, 0.7 mM $NaNO_3$) supplementation. Error bars indicate SEM. * = main effect. Orange (*) symbols = nitrate effect; black (*) symbols = PPARα effect. 1 (*) symbol = $p < 0.05$; 3 (***) symbols = $p < 0.001$. Symbols in brackets (e.g. $^{(*)}$) denote significance of a test of a combination of groups (i.e. main effects or two-way interactions) as described in the text. $n$ = 8-10 per group.